

Geomagnetic Variation and Field-Aligned Currents at Northern High-Latitudes, and their Relations to the Solar Wind Parameters

A. E. Levitin, R. G. Afonina, B. A. Belov and Ya. I. Feldstein Izmiran

Phil. Trans. R. Soc. Lond. A 1982 **304**, 253-301

doi: 10.1098/rsta.1982.0013

Email alerting service

Receive free email alerts when new articles cite this article - sign up in the box at the top right-hand corner of the article or click [here](#)

To subscribe to *Phil. Trans. R. Soc. Lond. A* go to: <http://rsta.royalsocietypublishing.org/subscriptions>

GEOMAGNETIC VARIATION AND FIELD-ALIGNED CURRENTS AT NORTHERN HIGH-LATITUDES, AND THEIR RELATIONS TO THE SOLAR WIND PARAMETERS

BY A. E. LEVITIN, R. G. AFONINA, B. A. BELOV AND YA. I. FELDSTEIN
IZMIRAN, *Akademgorodok, Moscow Region, U.S.S.R.*

(Communicated by Sir David Bates, F.R.S. – Received 28 July 1980 – Revised 9 June 1981)

CONTENTS

PAGE

1.	INTRODUCTION	254
2.	FORMULATION OF THE PROBLEM	255
3.	SPACE–TIME DISTRIBUTIONS OF THE GEOMAGNETIC FIELD VARIATIONS	259
3.1.	Equivalent current systems	259
3.1.1.	Equivalent current system $I_{\text{eq}}(K^{B_y} > 0)$	259
3.1.2.	Equivalent current system $I_{\text{eq}}(K^{B_z})$	260
3.1.3.	Equivalent current system $I_{\text{eq}}(K^{B_x})$	262
3.1.4.	Equivalent current system $I_{\text{eq}}(H_{01})$	262
3.1.5.	Equivalent current systems controlled by the parameters of the solar wind plasma	263
3.1.6.	Equivalent current system $I_{\text{eq}}(K^{B_y})$	266
3.1.7.	Current system of residual variation of the geomagnetic field	267
3.2.	Simulation of the hourly-mean values of geomagnetic field variation	267
3.3.	Reconstruction of the hourly-mean values of B_y and B_z	269
4.	SPACE–TIME DISTRIBUTIONS OF THE FIELD-ALIGNED CURRENTS	271
4.1.	Methods of calculation	271
4.2.	Space–time distribution of the field-aligned currents $j_{\parallel}(H_{01})$ (summer season)	271
4.3.	Space–time distribution of the field-aligned currents $j_{\parallel}(K^{B_z} < 0)$	273
4.4.	Space–time distribution of the field-aligned currents $j_{\parallel}(K^{B_y} > 0)$	274
4.5.	Space–time distribution of the field-aligned currents $j_{\parallel}(K^{B_z} > 0)$	275
4.6.	Space–time distribution of the field-aligned currents controlled by parameters of the solar wind plasma	276
4.7.	A model of the field-aligned currents	277
5.	ANALYSIS OF THE FIELD-ALIGNED CURRENT MEASUREMENTS OF THE TRIAD AND ISIS SATELLITES	280
5.1.	Analysis of TRIAD passes through the day-cusp region	280
5.2.	Analysis of TRIAD satellite passes crossing the auroral oval	283
5.3.	Analysis of ISIS-2 passes	288
6.	DISCUSSION	289
	REFERENCES	299

By using statistical analysis to study the relation between the interplanetary and geomagnetic fields, geomagnetic variations have been detected that are controlled by different parameters of the solar wind. The equivalent current systems for these geomagnetic variations have been determined for the 1968 summer and winter seasons from data from 14 high latitude stations. It has been shown that the geomagnetic field at high latitudes ($\Phi \geq 60^\circ$) can be represented by a sum of fields controlled by components of the Interplanetary Magnetic Field (I.M.F.) and by the velocity and density of the solar wind plasma. A correlation model is proposed by means of which hourly-mean values of the three components (X, Y, Z) of the geomagnetic field vector at high latitudes may be determined from hourly-mean values of the components B_x, B_y and B_z of the I.M.F.

The space-time distribution of field-aligned currents has been reconstructed from the horizontal component of the ground level geomagnetic field variation. The correlation model of field-aligned currents has been obtained for high latitudes ($\Phi \geq 60^\circ$). According to the model the value and direction of the field-aligned current j_{\parallel} are determined by I.M.F. components and spatial coordinates. The proposed model of field-aligned currents enables the nature of the actual magnetic disturbance registered during a given pass of the TRIAD and ISIS-2 satellites through the high latitude region to be interpreted. Moreover it enables some discrepancies between observations and the models of field-aligned currents proposed in the literature to be understood.

1. INTRODUCTION

The main magnetospheric phenomena are the plasma convection and the electric fields and currents. They have been discussed by Axford (1969), Akasofu (1977), Boström (1964, 1975), Crooker (1979), Gurevich *et al.* (1976), Lyatsky (1978), Mozer *et al.* (1974), Nishida (1978), Pudovkin (1974), Pudovkin & Semenov (1977), Rostoker & Boström (1976), Stern (1977), Vasiliunas (1970), Volland (1973, 1975) and Wolf (1975). Magnetospheric convection can be induced in part by the electric field of the solar wind which is given by $E = -c^{-1}(v \times B_s)$, where v is the solar wind velocity and B_s is the southward component of the Interplanetary Magnetic Field (I.M.F.) penetrating into the magnetosphere. This occurs owing to reconnection of the geomagnetic and interplanetary fields (Dungey 1961; Nishida 1971; Stern 1973), and to viscous friction when the boundary layer of magnetospheric plasma is in motion (Axford & Hines 1961; Axford 1964). It can also be induced by the azimuthal (B_y) component of the I.M.F. (Lyatsky 1978; Nishida 1971, 1975; Stern 1973).

If the I.M.F., and the velocity (v) and density (n) of the solar wind are actually related to electric fields inside the Earth's magnetosphere, they should control the geomagnetic field variations in the high latitude zone, especially in the polar cap, i.e. inside the auroral oval. Experimental evidence of a relation between geomagnetic variations on the Earth's surface and solar wind parameters is presented by Akasofu (1979*a, b, c*), Arnoldy (1971), Burton *et al.* (1975), Caan *et al.* (1977), Feldstein (1976), Friis-Christensen *et al.* (1972), Foster *et al.* (1971), Hirshberg & Holzer (1975), Ivanov & Mikerina (1973, 1974), Kamide & Akasofu (1974), Kane (1976); Kawasaki *et al.* (1973), Kuznetsov & Troshichev (1977), Langel (1975), Maezawa (1976*a, b*, 1978), Mansurov (1969), Mansurov & Mansurova (1973), McPherron *et al.* (1973*a, b*), Mishin (1977, 1978), Nishida (1968, 1971), Nishida & Kokubun (1971), Perreault & Akasofu (1978), Rostoker (1978), Russell (1973), Sergeev (1977), Sumaruk & Feldstein (1973, 1975), Sumaruk *et al.* (1974), Svalgaard (1968, 1973, 1977), Troshichev (1975), Troshichev & Tsiganenko (1979) and Troshichev *et al.* (1979). Studies of the interrelation of I.M.F. components

(B_x, B_y, B_z) and geomagnetic field variations in the near-pole region showed that in the generation of variations on the Earth's surface the main role is played by the vertical (B_z) and azimuthal (B_y) I.M.F. components. Numerous observations in the polar region (performed by means of balloons, rockets and satellites) confirmed the close connection of various phenomena with the orientation of the I.M.F. (see review by Fairfield 1977).

A specific role in the complex magnetosphere-ionosphere system is played by magnetosphere-ionosphere currents; their theoretical study has a long history which is partially reflected in the papers by Boström (1964), Gurevich *et al.* (1976), Iwasaki & Nishida (1967), Jaggi & Wolf (1973), Kamide & Matsushita (1979*a, b*), Lyatsky & Maltsev (1972, 1975), Lyatsky *et al.* (1974*a, b*), Lyatsky (1978), Pudovkin (1975), Rostoker & Boström (1976), Stern (1977), Tverskoy (1968), Vasiliunas (1970, 1972), Volland (1973, 1975), Wolf (1970, 1974, 1975) and Yasuhara *et al.* (1975). It is assumed that the field-aligned currents are also important in energy transfer from the external regions of the magnetosphere, where interactions with solar wind and the I.M.F. occur, to the ionosphere of the polar cap (Feldstein *et al.* 1982) and of the auroral zone.

The transverse magnetic disturbances, related to the field-aligned currents, were frequently observed by the 1968-38C, ATS, OGO-5, TRIAD, ISIS-2 and S3-3 satellites (Burrows *et al.* 1976, 1978; Cattell *et al.* 1979; Coleman & McPherron 1970; Cummings *et al.* 1968; Fairfield & Ness 1972; Fairfield 1973; Iijima & Potemra 1976*a, b*, 1978; Iijima *et al.* 1978, 1979; McDiarmid *et al.* 1977, 1978*a, b*, 1979*a, b*; Meng & Akasofu 1969; Mozer *et al.* 1980; Potemra 1979; Potemra *et al.* 1979; Rostoker *et al.* 1975; Saflekos *et al.* 1978, 1979; Sugiura 1975, 1976; Zmuda *et al.* 1970 and Zmuda & Armstrong 1974).

2. FORMULATION OF THE PROBLEM

In this study our aims were fourfold: (a) to study the structure of geomagnetic variations: by using the method of regression analysis, to obtain quantitative relations connecting hourly-mean values of geomagnetic field components at $\Phi \gtrsim 60^\circ$ with plasma and magnetic field parameters in the solar wind (B_y, B_z, B_x, n, v, T_p) (T_p being the proton temperature); (b) for various types of geomagnetic variations on the ground, to obtain three-dimensional current systems in the upper atmosphere: equivalent current systems flowing over a spherical shell at the height of the ionosphere and field-aligned currents flowing into and out of the ionosphere; (c) to verify the accuracy of the simulation, based on the obtained correlations, of hourly-mean values of the three components of the vector of geomagnetic field variations at latitudes $\Phi \gtrsim 60^\circ$; (d) to compare the obtained model of space-time variations of field-aligned currents with the actual measurements of these currents made by the TRIAD and ISIS-2 satellites.

For statistical regression analysis magnetic observatories in northern high-latitudes, $\Phi \gtrsim 60^\circ$, were chosen; details of these observatories are presented in table 1.

The studies were made for the 1968 summer (May-August) and winter (January, February, November, December) seasons (the maximum of the twentieth cycle of solar activity). Hourly values of geomagnetic field components were transformed to the system of corrected geomagnetic coordinates (X increasing in the direction of the corrected geomagnetic pole; Y increasing eastwards; Z increasing downwards).

Data on solar plasma and the I.M.F. were used in the form of hourly-mean values. The components of the I.M.F. (B_x, B_y, B_z) (King 1975) were taken in the solar-ecliptic coordinate

system. The correlation was realized for hourly-mean values of plasma data, and interplanetary and geomagnetic fields measured at the same Universal Time (U.T.).

The linear correlation analysis was performed in the following stages.

(a) By using the least-squares method for each hour U.T. and for each observatory, equations of linear regression were obtained in the form

$$H_{\text{E}}^i = K_i^{B_y} B_y + H_0^{iB_y}, \quad (1)$$

where H_{E}^i are hourly-mean values of the components (X, Y, Z) of the geomagnetic field variations for a certain hour U.T. at each station i , and $H_0^{iB_y}$ are geomagnetic field variations independent of B_y .

TABLE 1. OBSERVATORIES, THEIR COORDINATES AND LOCAL MAGNETIC MIDNIGHT IN U.T.

station	geographic coordinates		corrected geomagnetic coordinates		local midnight U.T.
	ϕ /deg	λ /deg	Φ /deg	A /deg	
Thule	76.6	291.3	86.0	38.1	03h00
Resolute Bay	74.7	265.1	84.3	306.0	08h00
Mould Bay	76.2	240.6	80.7	264.0	11h00
Godhaven	69.2	306.5	77.6	43.4	02h30
Baker Lake	64.3	264.0	75.1	320.4	07h00
Chelyuskin	77.7	104.3	71.3	173.9	17h00
Great Whale River	55.3	282.2	68.2	353.8	05h00
Dikson	73.5	80.4	67.9	154.7	18h00
College	64.9	147.8	64.9	260.3	11h00
Sodankylä	67.4	26.6	63.4	108.9	21h00
Welen	66.2	169.8	62.6	243.0	12h00
Meanook	54.6	246.7	62.5	301.2	08h00
Sitka	57.1	224.7	59.8	276.6	10h00
Agincourt	43.8	280.7	57.2	350.1	05h00

(b) By using equation (1), which gives a relation between the geomagnetic field and the B_y -component of the I.M.F., dependence on the latter was eliminated from all the initial geomagnetic data. Regression equations were then deduced for the new set of data giving a relation between geomagnetic components and the B_z -component of the I.M.F.:

$$H_{\text{E}}^{i'} = K_i^{B_z} B_z + H_0^{iB_z}, \quad (2)$$

where $H_0^{iB_z}$ are geomagnetic field variations independent of B_z .

(c) By using equation (2), a dependence on the B_z -component of the I.M.F. was eliminated from the new set of data. From the residual (after double elimination) set of data, regression equations were obtained giving a relation between geomagnetic field components and the B_x -component of the I.M.F.:

$$H_{\text{E}}^{i''} = K_i^{B_x} B_x + H_{01}^i, \quad (3)$$

where H_{01}^i are the geomagnetic field variations independent of the I.M.F.

When determining the equations of linear regression, all operations were done separately for two sets of data:

- a set of ground-based X -, Y - and Z -components for $B_z > 0$;
- a set of ground-based data for $B_z < 0$.

The separation of the initial data into two sets (depending on the sign of B_z) was necessary to take into account differences in quantitative dependences of geomagnetic field variations

on B_y for different orientations of B_z (Friis-Christensen & Wilhelm 1975; Maezawa 1976*a*), and to include the possibility of different effects of positive and negative B_z -values on the character of geomagnetic variations in the polar cap (Horwitz & Akasofu 1979; Kuznetsov & Troshichev 1977; Rezhnev *et al.* 1980; Shelomentsev & Suche-Bator 1976; Sumaruk & Feldstein 1977). Moreover, the geometry of the magnetosphere changes slightly depending on the sign of B_z . This variation, affecting the character of the relation between I.M.F. components and magnetic field variations on the ground, is included, to a first approximation, by separating all available data into the two sets (*a*) and (*b*). Similarly, a comparison of geomagnetic variations that are independent of the I.M.F. for the two sets of data allows us to verify the reliability of the relations obtained between the geomagnetic field at high latitudes and the solar wind parameters.

Variations of all the parameters of the regression equations were examined. The regression coefficients $K_i^{P_y}$, $K_i^{P_z}$ and $K_i^{P_x}$ describe the response of the components of the geomagnetic field vector to a variation of 1 nT in B_y , B_z and B_x . The space-time distribution of $K_i^{P_y}$, $K_i^{P_z}$ and $K_i^{P_x}$ in the system, corrected geomagnetic latitude (Φ) and local geomagnetic time (M.L.T.) serve as a basis for the construction of elementary equivalent current systems. These are generated in the magnetosphere by the interaction of the geomagnetic field with the various I.M.F. components. It is assumed that the currents are located at the height of the ionospheric E-layer. The value and direction of the equivalent current system is then completely determined by the corresponding components of the I.M.F.

Use of the regression coefficients to obtain the equivalent current system eliminates the necessity of choosing a reference level to determine geomagnetic field variations.

The H_{01}^i -values represent geomagnetic field variations independent of the I.M.F. To obtain the corresponding equivalent current system that characterizes the solar wind interaction with the geomagnetosphere in the absence of the I.M.F. a reference level for geomagnetic field variations must be introduced. For the winter season, the following two levels were used: (*a*) daily-mean field values for winter quiet days, including secular variations; (*b*) the field values for winter quiet days at around midnight (M.L.T.) for polar cap stations and around midday (M.L.T.) for auroral zone stations, including the secular variations. For the summer season, the two corresponding levels were found by interpolation.

In some studies, higher values were obtained for the correlation coefficients r of the activity indexes (K_p , AE) with the electric field E of the solar wind than with the I.M.F. components. A study made by Afonina *et al.* (1975), however, has shown that r -values connecting the geomagnetic field at the near-polar observatory Resolute Bay with B_y and $E = -c^{-1}(v \times B_y)$ are practically identical. An additional study made by using data from the Thule, Cape Chelyuskin and College Observatories for the 1968 summer season showed that for the three components of geomagnetic field the values of r are practically identical (within the limits of the error in r) for the relations of the ground-based components both with B_y and $-c^{-1}(v \times B_y)$, and with B_z and $-c^{-1}(v \times B_z)$, for B_z both more than and less than zero. In the subsequent analysis of the high latitude field variations the components of the I.M.F. were therefore used instead of the E -components. When using E as the controlling parameter, $K_i^{P_j}$ -coefficients in the regression equations are decreased by a factor of \bar{v} , where \bar{v} is the average value of the solar wind velocity.

According to Russell & Rosenberg (1974) the component of the I.M.F. that controls the special type of near-pole variations is the B_y -component in the solar-magnetospheric (SM) coordinate system, but according to Kawasaki *et al.* (1973) there is a closer correlation with

B_y in the solar-ecliptic (SE) system. It was shown by Afonina *et al.* (1975) that the correlation coefficients r_{SE} , r_{SM} of the components of the field variations on the ground for the summer season in Resolute Bay with B_y in different coordinate systems are equal within the limits of error in r . Recount of B_y to different coordinate systems was made (cf. Russell 1971). More detailed analysis indicates that application of different coordinate systems may result in some redistribution of the coefficients in the regression equations between various I.M.F. components if one uses the solar-magnetospheric system. Separate analyses in solar-ecliptic and solar-magnetospheric coordinate systems for five near-polar observatories showed that in the summer and winter seasons the choice of the coordinate system is not of great importance (Troshichev & Tsiganenko 1979).

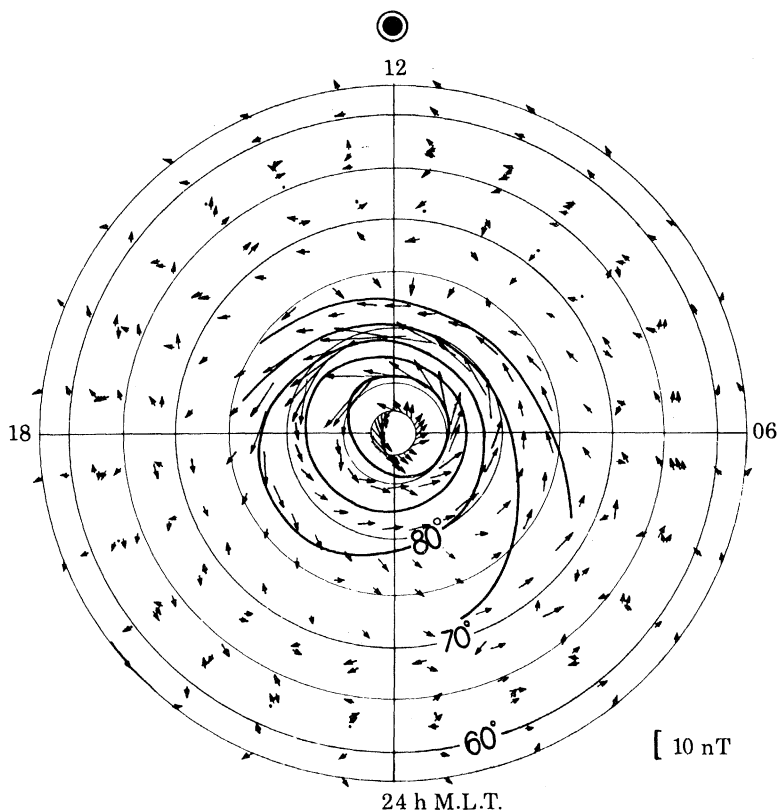


FIGURE 1. Equivalent current system $I_{eq}(K^{B_y > 0})$ for the 1968 summer reflecting a relation between geomagnetic field variations and B_y for a variation in B_y of $+1$ nT for $B_z > 0$. A current of 5 kA flows between isolines. Arrows in this and subsequent figures representing current systems show current vectors for every hour M.L.T. from the data of the fourteen stations listed in table 1. The scale in the lower right corner is for geomagnetic field vectors. These vectors can be transformed into current vectors by turning the scale clockwise through 90° .

Geomagnetic field variations independent of the I.M.F. appeared to be connected with the parameters n , v , T_p of the solar wind plasma. For the 1968 summer season it was possible to select some sets of statistically mutually independent parameters. One of these sets is B_y , B_z , $nv^2 \propto nT_p$; v^2 . Therefore, from the variation independent of the I.M.F., the parts controlled by nv^2 and v^2 were separated. Thus, the expansion may be written in the general form

$$H_E^i = K_i^{B_y} B_y + K_i^{B_z} B_z + K_i^{B_x} B_x + K_i^{nv^2} n \left(\frac{1}{100} v\right)^2 + K_i^{v^2} \left(\frac{1}{100} v\right)^2 + K_i^{|B_y|} |B_y| + H_0^i. \quad (4)$$

3. SPACE-TIME DISTRIBUTIONS OF THE GEOMAGNETIC FIELD VARIATIONS

3.1. Equivalent current systems

3.1.1. Equivalent current system $I_{eq}(K^{B_y > 0})$

The values of $K_i^{B_j}$ characterizing the value of the magnetic field variation per unit variation of the various interplanetary-medium parameters have been given by Afonina *et al.* (1979a) and Belov *et al.* (1977). In figure 1, for the set of data with $B_z > 0$, the equivalent current system $I_{eq}(K^{B_y > 0})$ is presented. It reflects a relation between geomagnetic field variations and B_y for a B_y -variation of 1 nT for the 1968 summer. A similar current system exists for the set of data with $B_z < 0$.

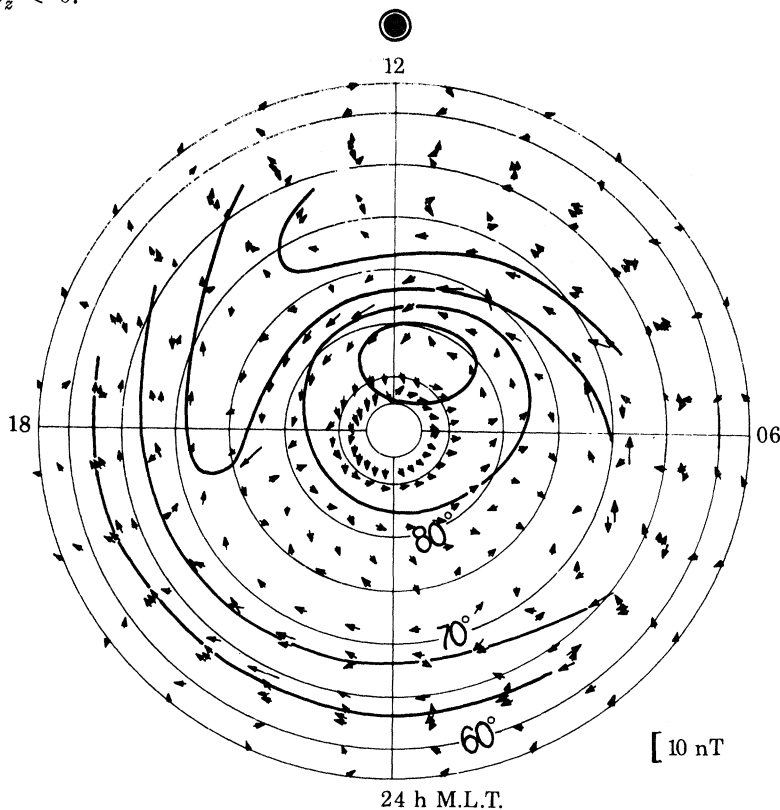


FIGURE 2. Equivalent current system $I_{eq}(K^{B_y > 0})$ for the 1968 winter. A current of *ca.* 1.5 kA flows between isolines.

Independently of the sign of B_z , the current system controlled by B_y is characterized by the presence of a zonal current directed counterclockwise (with a variation in B_y of -1 nT, the current direction will be reversed) with maximum intensity in the daytime sector at latitudes 80 – 84° for $B_z > 0$ and 77 – 80° for $B_z < 0$. The field variations controlled by B_y in auroral and subauroral latitudes in the summer are small and comparatively irregular. The concentration of current lines of the equivalent current system could be interpreted as the appearance of a polar electrojet, so called in comparison with the auroral electrojets located along the auroral oval.

Figure 2 represents the equivalent current system $I_{eq}(K^{B_y > 0})$ similar to that in figure 1 but for the 1968 winter season. The winter current system controlled by B_y , as well as the summer system for either sign of B_z , is characterized by an intensified counterclockwise zonal current in

the daytime sector. (With a change of sign of B_y , the current direction is reversed.) For $B_z < 0$, the region with an intensified zonal current is expanded to include lower latitudes. The most intense current is observed at lower latitudes in winter ($75^\circ \lesssim \Phi \lesssim 77^\circ$) than in summer and occurs between 09 h and 14 h M.L.T. A concentration of current lines in the daytime sector in the region $75^\circ \lesssim \Phi \lesssim 77^\circ$ indicates the presence of a greatly weakened near-polar electrojet in the winter season too. The latitudinal poleward shift of the jet between winter and summer is about 4° . The intensity of the total equivalent current in the winter polar cap is about one fifth that in the summer cap. The characteristic feature of the winter equivalent current system $I_{\text{eq}}(KB_y > 0)$ is the appearance of the westward current (or the eastward current for $B_y < 0$) from 19 h to 03 h M.L.T. at latitudes $62^\circ \lesssim \Phi \lesssim 68^\circ$. The current intensity is comparable with that of the winter polar electrojet and is substantially larger in the early morning at $\Phi \approx 68^\circ$ for $B_z < 0$ than for $B_z > 0$.

3.1.2. Equivalent current system $I_{\text{eq}}(KB_z)$

The equivalent current system $I_{\text{eq}}(KB_z < 0)$ for the summer season is presented in figure 3*a*. It characterizes the response of the geomagnetic field to a decrease in B_z by -1 nT for $B_z < 0$. The current system consists of a current distributed throughout the polar cap, flowing, on average, along the 21 h–09 h M.L.T. meridian and closing through lower latitudes. Concentration of the current lines at the latitudes of the auroral zone reflects the presence of two auroral electrojets in the westward and eastward directions. These are the general elements of the current system controlled by $B_z < 0$. The westward electrojet flows in the morning and night sectors and has maximum intensity (*ca.* 60 kA) at 02 h–05 h M.L.T. The eastward electrojet is located in the evening sector and has maximum intensity (*ca.* 30 kA) at 15 h–17 h M.L.T. Towards the lower latitude the intensity of the electrojet decreases from its maximum value at $\Phi \approx 68^\circ$. At $\Phi \approx 57^\circ$ the intensity is so small that it is doubtful whether there is a current outflow from the auroral zone to mid-latitudes.

The current system $I_{\text{eq}}(KB_z < 0)$ for the winter season is presented in figure 3*b*. This system is formed by one current vortex with a clockwise current distributed over the whole high latitude region. The difference in intensities of the westward auroral electrojet in winter and summer is negligible. The ratio of current intensity in the westward electrojet to that in the near-pole region in the daytime is changed owing to a substantial decrease of the intensity of daytime disturbances. The ratio is equal to two in the summer season, whereas in winter it is equal to four. The polar cap current is rotated through about 45° in the clockwise direction with respect to that in the summer season. The eastward electrojet in the evening sector, which is pronounced in the summer season, practically vanishes in winter.

The equivalent current system $I_{\text{eq}}(KB_z > 0)$ is shown in figure 4. It presents the response of the geomagnetic field during periods when $B_z > 0$ to a variation in B_z of 1 nT for the summer season. The equivalent current flows through the near-pole region from the day- to the night-side, i.e. the current flows in the opposite direction to that presented in figure 3 for $B_z < 0$. The equivalent current through the near-polar region, most intense in the near-noon sector, is closed through the lower latitudes forming two vortices with the foci at *ca.* 09 h and *ca.* 15 h M.L.T. The focus of the afternoon vortex with the clockwise current is located at a higher latitude ($\Phi \approx 84^\circ$) than that of the pre-noon vortex ($\Phi \approx 80^\circ$). The current system controlled by $B_z > 0$ is located at $\Phi > 70^\circ$. Its contribution to the generation of geomagnetic disturbances at auroral and subauroral latitudes is negligible.

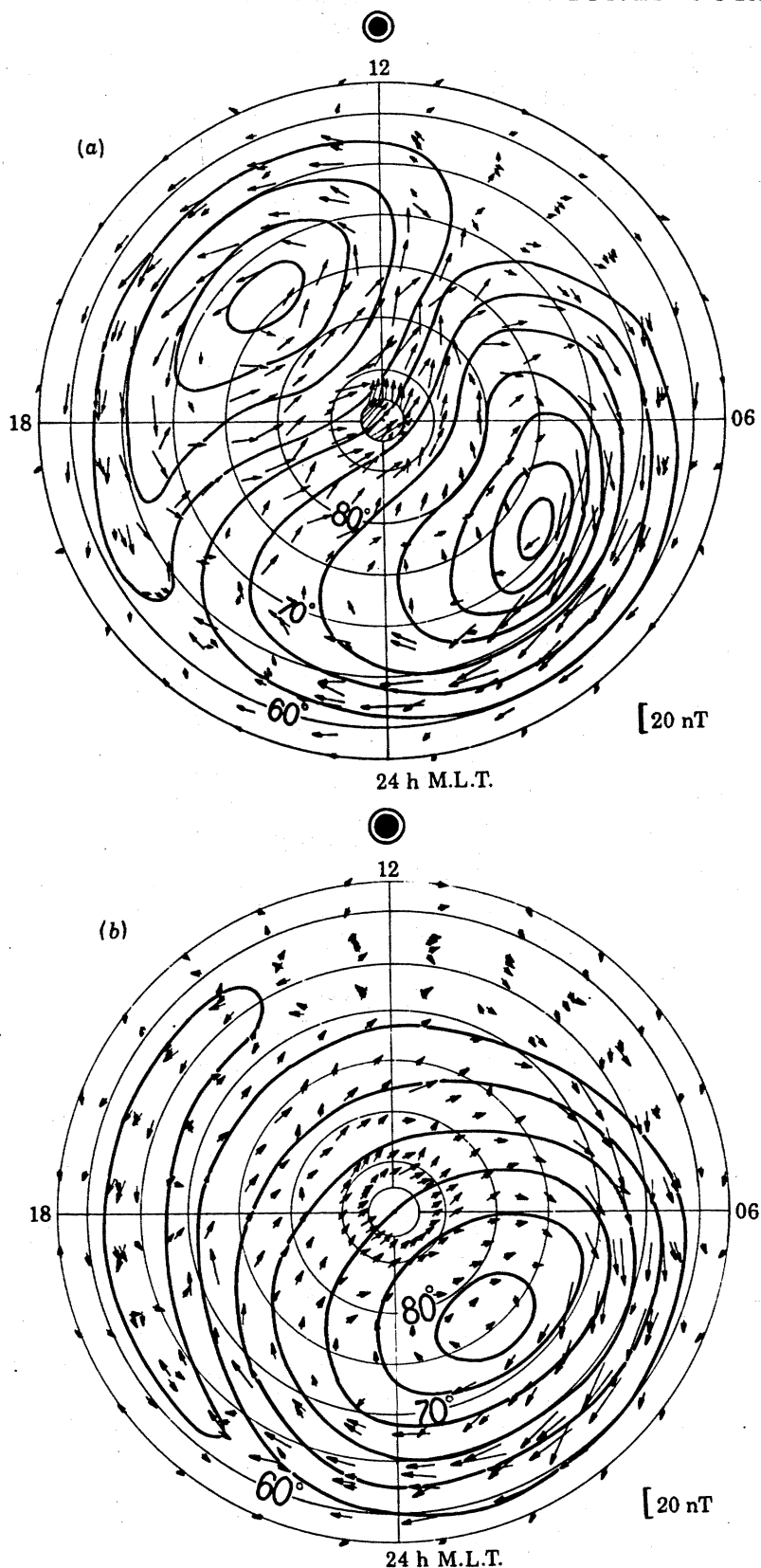


FIGURE 3. Equivalent current systems $I_{eq}(K^{B_z < 0})$ reflecting a relation between the geomagnetic field variations and the $B_z < 0$ component of the I.M.F. for a variation in B_z of -1 nT: (a) the 1968 summer; a current of 8 kA flows between isolines; (b) the 1968 winter; a current of ca. 5 kA flows between isolines.

The current intensity in the near-pole region for winter is about one fifth that for summer. The total intensity decreases in approximately the same way. Furthermore, the focus of the pre-noon vortex in the winter polar cap is shifted toward earlier hours (04 h–05 h M.L.T.) than that of the summer, and the focus of the afternoon vortex is located at lower latitudes ($\Phi \approx 79^\circ$).

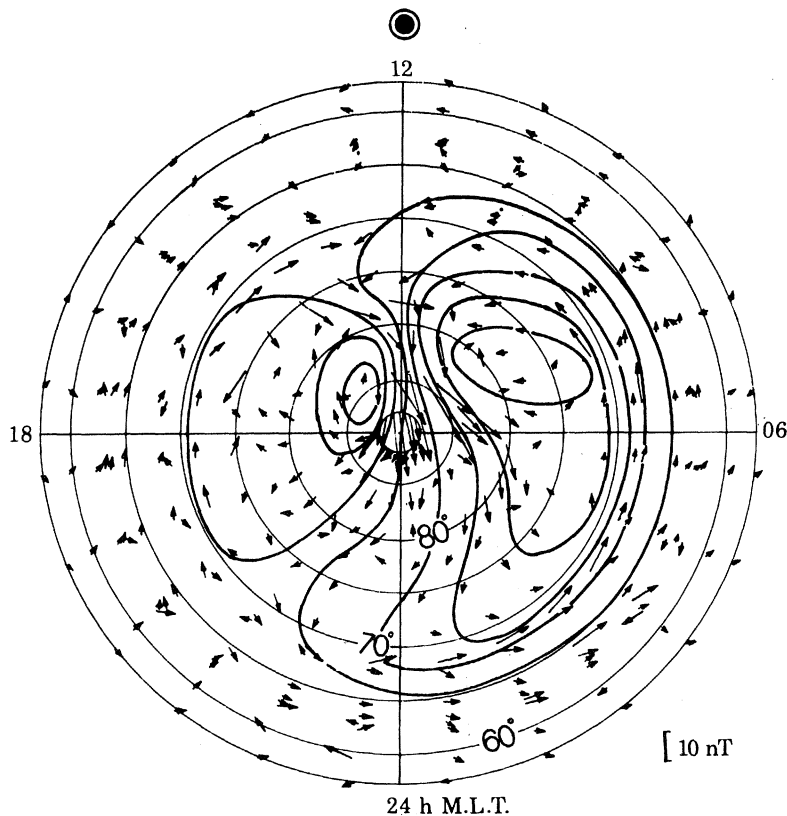


FIGURE 4. Equivalent current systems $I_{\text{eq}}(K^{B_z > 0})$ representing a relation between the geomagnetic field variations and the $B_z > 0$ I.M.F. component for a variation in B_z of +1 nT for the 1968 summer. A current of ca. 4 kA flows between isolines.

3.1.3. Equivalent current system $I_{\text{eq}}(K^{B_x})$

The current systems related to B_x are not presented in this paper. They are weak for both summer and winter seasons. Such an effect was revealed by Burch & Heelis (1979) for other geophysical phenomena. As far as we know from the literature there is no current system that would be controlled by B_x . The contribution of B_x is reflected in the rotation of the two-vortex current system by a certain angle (Mishin 1978; Stern 1973). The coefficients $K_i^{B_x}$ calculated by Afonina *et al.* (1975, 1979*a, b*) at some stations are sometimes considerable and are quite regular. It is necessary, however, to prove the existence of field variations controlled by B_x .

3.1.4. Equivalent current system $I_{\text{eq}}(H_{01})$

In figure 5 is presented the equivalent current system $I_{\text{eq}}(H_{01})$ independent of the I.M.F., for the data set for $B_z > 0$ for the 1968 summer season. This current system characterizes the

GEOMAGNETIC VARIATIONS AND FIELD-ALIGNED CURRENTS 263

field variations at average values of solar wind density, $\bar{n} \approx 4$ particles cm^{-3} , and velocity, $\bar{v} \approx 500$ km s^{-1} .

The equivalent current system independent of the I.M.F. consists of a current in the polar cap that flows from the night- to the dayside and forms two vortices. Not all of the current lines are enclosed within the limit $\Phi \gtrsim 60^\circ$; this indicates a contribution independent of the I.M.F. current system to field variations at mid-latitudes.

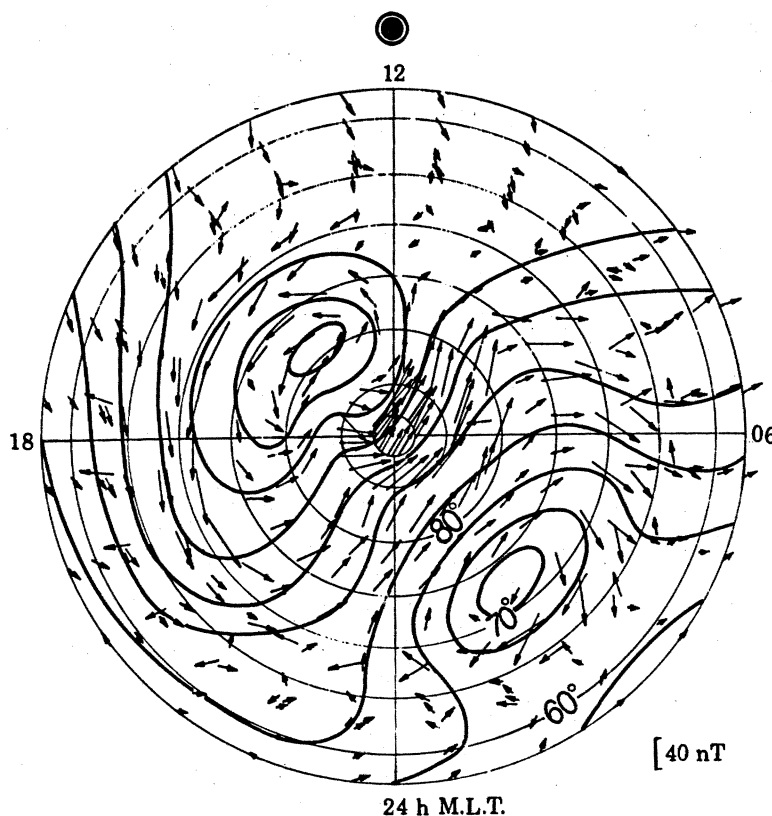


FIGURE 5. Equivalent current system $I_{\text{eq}}(H_{01})$ for geomagnetic variations independent of the I.M.F. for the 1968 summer ($B_z > 0$). A current of 30 kA flows between isolines.

In constructing the equivalent current system presented in figure 5, the daily-mean values of quiet winters, interpolated with the inclusion of the secular variations to the 1968 summer, were taken as the reference level. The intensity relations of two-current vortices are actually different in the winter and summer seasons. Whereas in the summer current system, $I_{\text{eq}}(H_{01})$, the day-evening vortex is more intense, in the winter system the morning vortex is more intense.

For the polar cap, the equivalent current systems, both controlled by and independent of the I.M.F., were obtained by Troshichev & Tsiganenko (1979) and Troshichev *et al.* (1979) for the summer and winter seasons in the minimum of the solar activity cycle.

3.1.5. Equivalent current systems controlled by the parameters of the solar wind plasma

A relation between the magnetic field variations and v^2 and nv^2 results from theoretical considerations according to Axford (1979). The equivalent current systems have been obtained

from the regression coefficients $K_i^{v^2}$ and $K_i^{nv^2}$. Figure 6 represents the system $I_{eq}(K^{v^2})$ ($B_z > 0$) for the 1968 summer.

The equivalent current system in figure 6 has two vortices. The difference between the systems for $B_z < 0$ and for $B_z > 0$ is mainly in their intensity (the current for $B_z < 0$ is twice as intense as that in figure 6). Moreover, the maximum of the zonal eastward current is located several degrees further north for $B_z > 0$.

The equivalent current system $I_{eq}(K^{nv^2})$ dependent on nv^2 for $B_z > 0$ is presented in figure 7. The system consists of two vortices, with the current flowing from 22 h to 10 h M.L.T. in the polar cap.

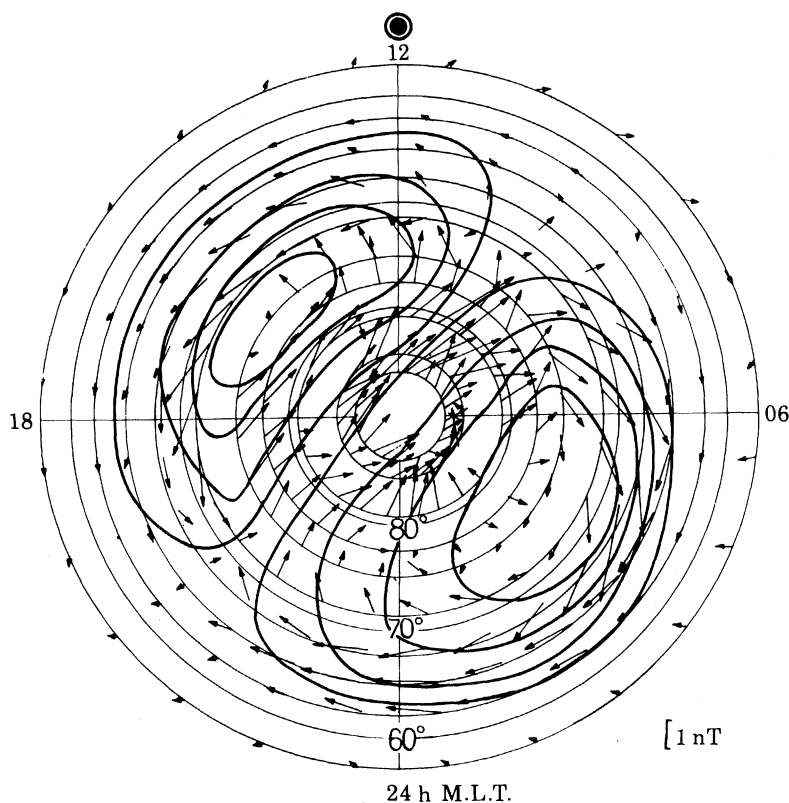


FIGURE 6. Equivalent current systems $I_{eq}(K^{v^2})$ reflecting a relation between the geomagnetic variations and the squared velocity of the solar wind for a variation in $(v/100)^2$ of 1 for $B_z > 0$. A current of *ca.* 1.5 kA flows between isolines.

In figure 8 is presented the equivalent current system $I_{eq}(K^{v^2}\bar{v}^2 + K^{nv^2}\bar{nv}^2)$ characterizing the cumulative effect of the parameters v^2 and nv^2 for the average values \bar{v}^2 and \bar{nv}^2 . This system represents, apparently, in the most pure form, the field variations controlled by the parameters of the solar wind plasma. It is practically coincident for average values in the 1968 summer with the current system presented in figure 5, which represents the field variations independent of the I.M.F. The differences between figure 8 and figure 5 are caused by the presence of field variations controlled by the absolute value $|B_y|$, related to the dynamo action of ionospheric winds and, possibly, to any other variations of the field contributing to the current system shown in figure 5.

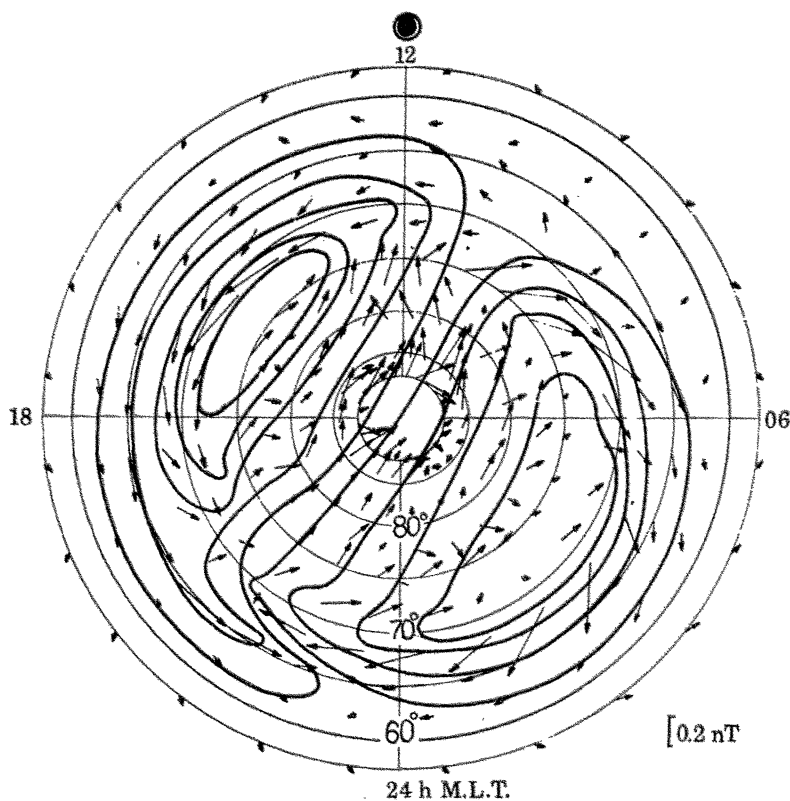


FIGURE 7. Equivalent current system $I_{\text{eq}}(K n^2)$ dependent on n^2 for a variation in $n(v/100)^2$ of 1 for $B_z > 0$. A current of ca. 0.1 kA flows between isolines.

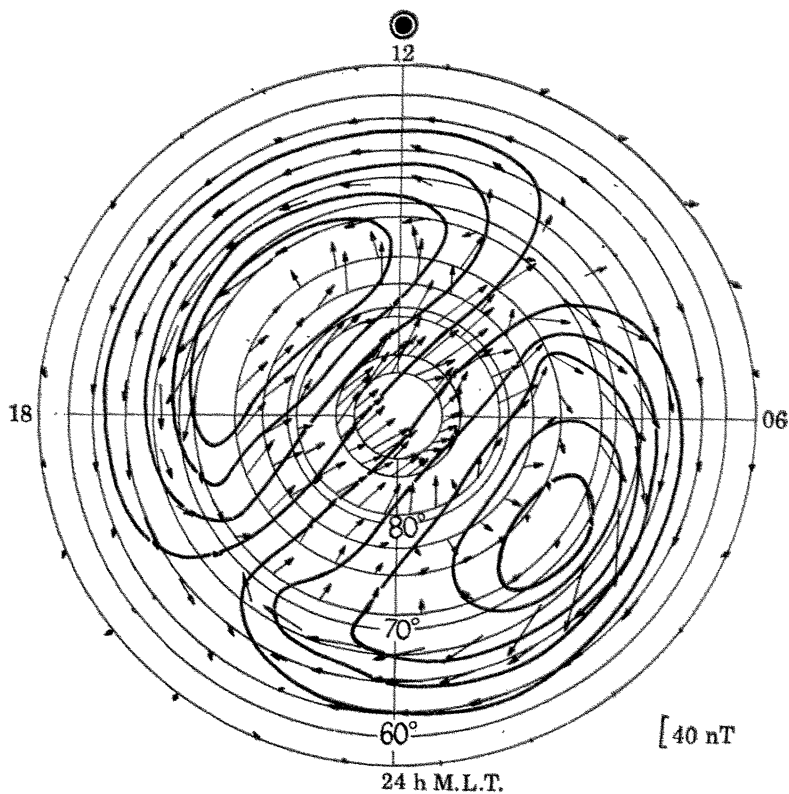


FIGURE 8. Equivalent current system $I_{\text{eq}}(K v^2 + K n^2 n v^2)$ for the average values of v^2 and $n v^2$ characterizing the resultant effect of v^2 and $n v^2$ for $B_z > 0$. A current of ca. 25 kA flows between isolines.

3.1.6. Equivalent current system $I_{\text{eq}}(K^{|B_y|})$

We noted in §3.1.5 the possibility of the existence of field variations in the polar cap controlled by $|B_y|$. Such a system was in fact obtained from the experimental data by Mishin (1978). The presence of the $K^{|B_y|}$ -variation should result in a difference in K^{B_y} for the sets of data with $B_y > 0$ and $B_y < 0$. To detect $|B_y|$ variations, the observations from nine observatories in the high latitude region $\Phi > 63^\circ$ were used. The values of the regression coefficients $K_i^{B_y}$ in (4) were determined separately for $B_y > 0$ and $B_y < 0$. The values of $K_i^{|B_y|}$ for the known $K_i^{B_y > 0}$ and $K_i^{B_y < 0}$ were determined from the relation

$$K_i^{|B_y|} = \frac{1}{2}(K_i^{B_y > 0} - K_i^{B_y < 0}).$$

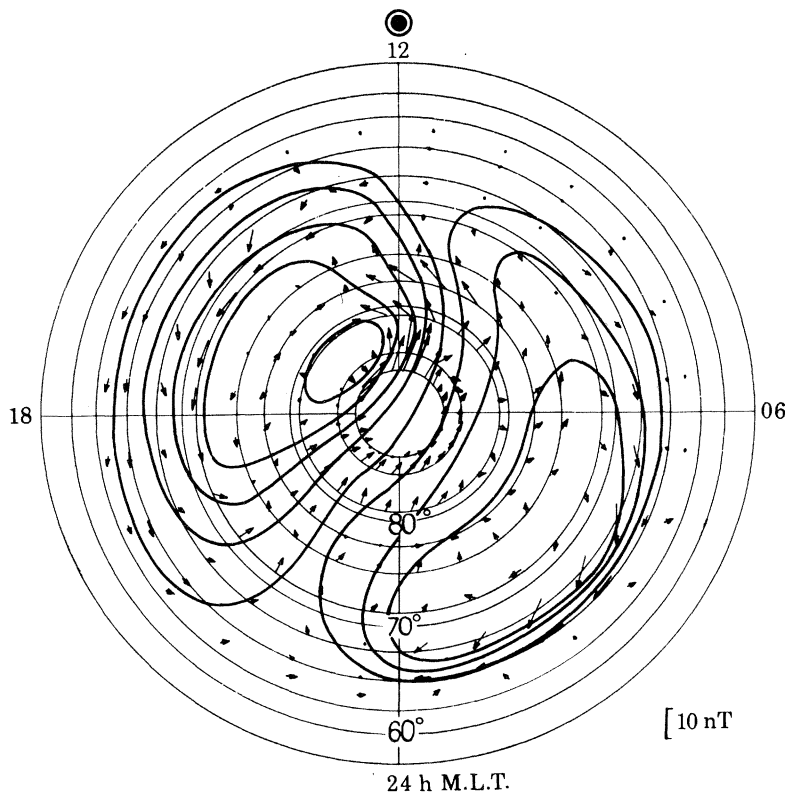


FIGURE 9. Equivalent current system $I_{\text{eq}}(K^{|B_y|})$, reflecting the effect of the absolute value, $|B_y|$, of the azimuthal I.M.F. component for $B_z > 0$. A current of ca. 3.5 kA flows between isolines.

Figure 9 shows the equivalent current system $I_{\text{eq}}(K^{|B_y|})$ for $B_z > 0$ for a variation in $|B_y|$ of 1 nT for the 1968 summer. The methods used by Mishin (1978) and in our work to detect a relation between the field variations and $|B_y|$ enable us to separate this relation only formally into its symmetric and asymmetric parts with respect to B_y . One can explain the results of such a separation in two ways: (a) by assuming both parts really exist owing to the different physical mechanisms of their generation; (b) by considering the symmetric part, controlled by $|B_y|$, as being the result of a change in the topology of the asymmetric part due to a change in the sign of B_y . It is almost impossible at present to make an unambiguous choice between the two interpretations; both variants can, however, be realized.

3.1.7. Current system of residual variation of the geomagnetic field

Expansion (4) contains, in addition to terms depending on the I.M.F. components and on the parameters of the solar wind plasma, the residual term H_0^i . The equivalent current system of the field variations described by this term as a deviation from daily-mean values is presented in figure 10 for the 1968 summer. The current system is characterized by the high-latitude current that flows into the region during the afternoon–evening and flows out during morning–pre-noon. The total current intensity is approximately one half that of the system in figure 5.

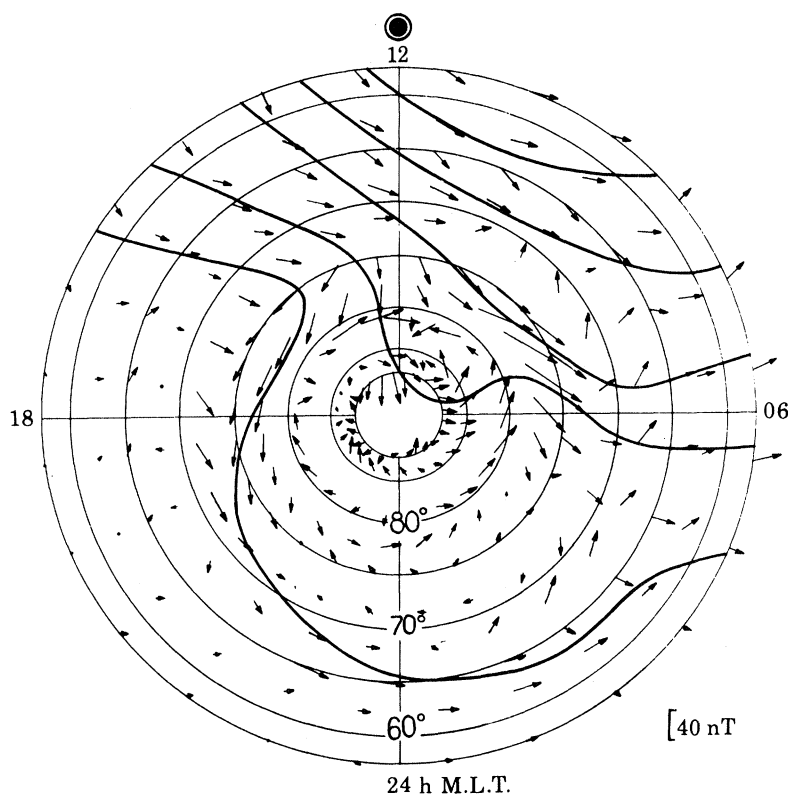


FIGURE 10. Equivalent current system $I_{eq}(H_0)$ for the 1968 summer characterized by the residual term H_0^i after elimination of the effects of the I.M.F. components and the solar wind plasma parameters. A current of ca. 50 kA flows between the isolines.

Although a part of the dispersion of the vectors can be explained by the accumulation of statistical errors in detecting five current systems related to the solar wind parameters, and by a problematic choice of the reference level (in particular, for the X -component), we can consider as satisfactory that the equivalent currents in figure 10 are assumed to be an extrapolation of mid-latitude S_q -currents to high latitude regions.

The current system is in satisfactory agreement with the neutral wind distribution in the high latitude ionosphere, obtained from observations of barium cloud drift by Meriwether *et al.* (1973).

3.2. Simulation of the hourly-mean values of geomagnetic field variation

The coefficients $K_t^{P_y}$, $K_t^{P_z}$, $K_t^{P_x}$ and the values H_{01}^i obtained as a result of correlation analysis enable us to calculate the three components of the vector of geomagnetic field variations at the

14 high latitude observatories listed in table 1 (Afonina *et al.* 1979*a*). Applying interpolation methods, one can calculate the magnetic field at points between neighbouring stations to describe the magnetic field variations over the whole high latitude region.

The accuracy of the model can be seen from figure 11 where the observed hourly-mean values of the X -component of the geomagnetic field vector (open circles) and the hourly-mean values obtained from the correlation model (closed circles) are given for the stations Thule, Resolute Bay, Mould Bay, Baker Lake, Chelyuskin, Dikson, College and Meanook for the 1968 summer and winter.

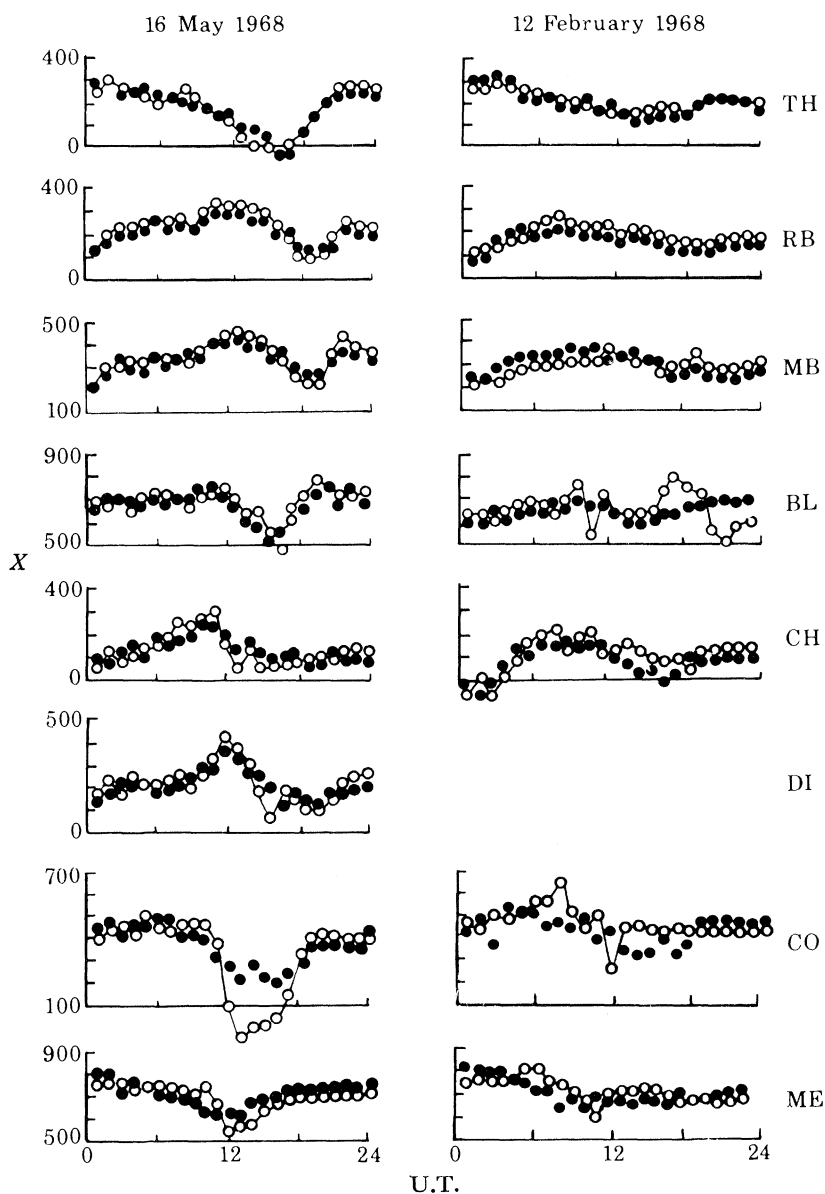


FIGURE 11. Hourly-mean values of the X -components of the vector of geomagnetic variations observed (\circ) and determined from the correlation model (\bullet) showing typical agreement between model and observations for the 1968 summer and winter. Data are presented for the stations Thule (TH), Resolute Bay (RB), Mould Bay (MB), Baker Lake (BL), Chelyuskin (CH), Dikson (DI), College (CO) and Meanook (ME) for 16 May and 12 February 1968.

We took 16 May 1968 as being characteristic of the adequacy of the model for summer. The mean-square dispersion of the calculated values from those observed is *ca.* 30 nT in the polar cap and *ca.* 50 nT in the auroral zone. Simulation of geomagnetic fields at high latitudes indicates that the linear correlation gives a satisfactory description of relations of these fields with the components except for substorms (Iyemori *et al.* 1979). The model, the input parameters of which are the hourly-mean values of the I.M.F. components, cannot simulate sub-storm activity. The proposed model gives the best agreement with observation at the latitudes of polar cap. This enables us to solve the inverse problem: to find the B_y and B_z I.M.F. components from the data from the observatory network in the polar cap. For the winter season, the agreement of the calculated values of geomagnetic field variations with the experimental values is substantially worse. We took 12 February 1968 as typical for the winter season. The calculations show that the seasonally dependent model enables us to determine the hourly-mean values of variations of geomagnetic field components at high latitudes with considerable accuracy in the absence of substorms.

3.3. Reconstruction of the hourly-mean values of B_y and B_z

Figure 12 gives examples of a reconstruction of the hourly-mean values of B_y and B_z for 16 and 17 May 1968. Open circles give observed values and the closed circles give the results of calculations according to the accepted model. As the relation between geomagnetic field variations on the ground and the radial I.M.F. component B_x is very weak, it seems to be impossible to find B_x with sufficient accuracy. By averaging over longer periods, agreement between reconstructed and observed values of the I.M.F. components is improved. For illustration, table 2 gives the values of the calculated and observed I.M.F. components for intervals of 3, 12 and 24 h for 16 and 17 May 1968.

All of the model parameters for the 1968 summer needed to determine the values of B_y and B_z are described by Afonina *et al.* (1979*a*). The method of restoration of B_y and B_z from the ground-based data is as follows. For each hour U.T., the equations

$$X = K_{\pm xy} B_y + K_{\pm xz} B_z + K_{xx} B_x + X_{\pm 0},$$

$$Y = K_{\pm yy} B_y + K_{\pm yz} B_z + K_{yx} B_x + Y_{\pm 0},$$

$$Z = K_{\pm zy} B_y + K_{\pm zz} B_z + K_{zx} B_x + Z_{\pm 0}$$

are used to calculate the magnetic field variations at the observatories where the coefficients K_{ny} or K_{mz} prevail, i.e. $|K_{ny}| \gg |K_{nz}|$ and $|K_{nx}|$ or $|K_{mz}| \gg |K_{my}|$ and $|K_{mx}|$. For example, in the 1968 summer for 19 h–20 h U.T. with $B_z > 0$: for the observatory Resolute Bay (RB) $K_{yz} = -31.9$, $K_{yy} = -1.1$, $K_{yx} = +3.4$; and for Mould Bay (MB) $K_{xy} = 31.9$, $K_{xz} = 6.1$, $K_{xx} = -0.6$. The preceding equations therefore take the form

$$Y_{\text{RB}} = 3.4 B_x - 1.1 B_y - 31.9 B_z + Y_{0\text{RB}},$$

$$X_{\text{MB}} = -0.6 B_x + 31.9 B_y + 6.1 B_z + X_{0\text{MB}},$$

which gives

$$B_y \approx \frac{X_{\text{MB}} - X_{0\text{MB}}}{31.9}; \quad B_z \approx \frac{Y_{\text{RB}} - Y_{0\text{RB}}}{-31.9}.$$

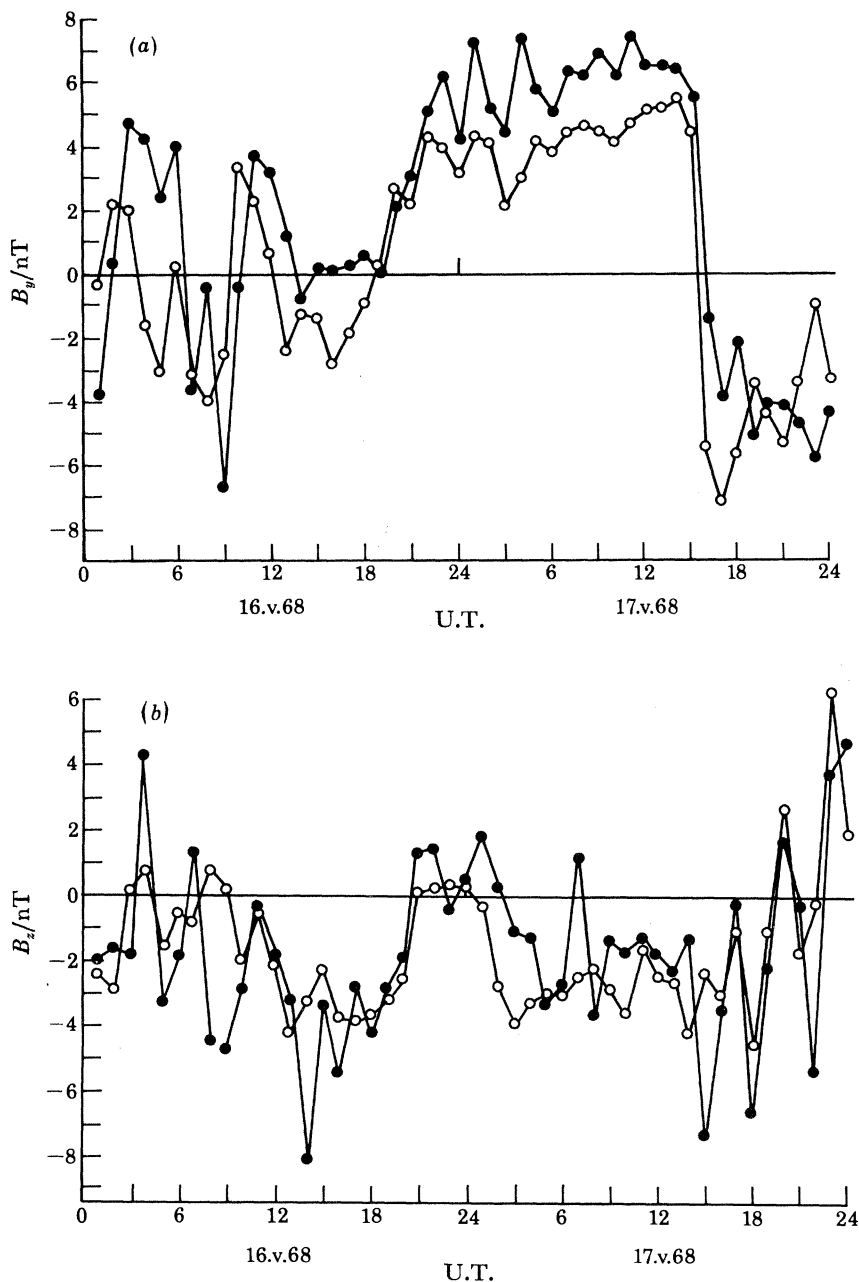


FIGURE 12. Examples of the reconstruction of hourly-mean values of (a) B_y and (b) B_z for 16 and 17 May 1968. Open circles correspond to experimental values and closed circles to values calculated according to the proposed model.

TABLE 2. OBSERVED AND CALCULATED VALUES OF B_y AND B_z (nT) FOR 16 AND 17 MAY 1968

	U.T./h	01-03	04-06	07-09	10-12	13-15	16-18	19-21	22-24	01-12	12-24	01-24
16 May	B_y (calc.)	0.4	3.5	-3.6	3.3	0.2	0.4	1.9	5.3	0.7	1.9	1.3
	B_y (obs.)	1.5	-1.4	-3.2	2.5	-1.7	-2.0	1.8	3.8	-0.1	0.5	0.2
	B_z (calc.)	-1.6	-0.3	-2.6	-1.7	-4.9	-4.1	-1.1	0.5	-1.5	-2.4	-2.0
	B_z (obs.)	-1.7	-0.4	0.1	-1.5	-3.6	-3.7	-1.8	0.3	-0.9	-2.2	-1.6
17 May	B_y (calc.)	5.7	6.2	6.6	6.9	6.7	-2.7	-4.3	-4.8	6.3	-1.3	2.5
	B_y (obs.)	3.6	3.7	4.6	4.8	5.1	-6.0	-4.3	-2.5	4.2	-1.9	1.2
	B_z (calc.)	0.3	-2.4	-1.2	-1.6	-3.7	-3.5	-0.2	0.8	-1.2	-1.7	-2.0
	B_z (obs.)	-2.4	-3.1	-2.5	-2.5	-3.0	-2.9	0.0	2.8	-2.6	-0.8	-1.7

The equations for the Resolute Bay and Baker Lake (BL) observatories (for 19 h–20 h U.T.) with $B_z < 0$ are

$$Z_{\text{RB}} = -1.4 B_x - 28.2 B_y + 0.5 B_z + Z_{0\text{RB}},$$

$$Y_{\text{BL}} = -0.3 B_x - 4.3 B_y - 21.8 B_z + Y_{0\text{BL}},$$

which gives

$$B_y \approx \frac{Z_{\text{RB}} - Z_{0\text{RB}}}{-28.2}; \quad B_z \approx \frac{Y_{\text{BL}} - Y_{0\text{BL}}}{-21.8}.$$

The data from observatories with the maximum values of K_{ny} and K_{mz} for a particular hour U.T. are used to calculate B_y and B_z for that hour. The most important characteristic of the proposed method is the choice of sign for B_z . Data from other observatories were used if their coefficients K_{ny} and K_{mz} were large and had comparable absolute values at a given hour U.T. to determine the sign of B_z more accurately. Application of the additional data enables us to derive the sign of B_z with the minimum difference between calculated and measured values of geomagnetic field components.

The reconstructed values of B_y and B_z , presented in figure 12, have been obtained by means of the method described. If there were a denser network of observatories in the polar caps, the reconstruction of the I.M.F. components could be made with more accuracy, and we would be able to reconstruct the values of B_y and B_z from ground-based observations at the summer polar cap. The model can be improved by studying its variations with the solar activity cycle.

4. SPACE-TIME DISTRIBUTIONS OF THE FIELD-ALIGNED CURRENTS

4.1. Methods of calculation

The analysis made it possible to separate the observed variations of the geomagnetic field at high latitudes into their components, (figures 1–10). The data on the space-time distribution of the horizontal vectors of a disturbed field allow us to calculate (making some assumptions) the space-time distribution of the field-aligned currents j_{\parallel} connected with a given geomagnetic variation. Calculations of vertical currents have been made based on the general theory developed by Gurevich *et al.* (1976). According to this theory

$$j_{\parallel} [A \text{ km}^{-2}] = \frac{10}{4\pi} \frac{\Sigma_{\text{P}}}{\Sigma_{\text{H}}} \text{div } H [\text{nT km}^{-1}], \quad (5)$$

where Σ_{P} and Σ_{H} are the integral Pedersen and Hall conductivities of the ionosphere respectively. Thus, by calculating a divergence of the horizontal vector H of a given geomagnetic variation, one can determine j_{\parallel} in the space cell under calculation. In the subsequent calculations, the longitudinal dimension of a cell was 15° (1 h M.L.T.) and the latitudinal dimension $\Delta\Phi$ was determined by the distribution of the magnetic observatories: $(57.2\text{--}59.8^{\circ})$, $(59.8\text{--}62.5^{\circ})$, $(62.5\text{--}64.9^{\circ})$, $(64.9\text{--}68.2^{\circ})$, $(68.2\text{--}71.3^{\circ})$, $(71.3\text{--}75.1^{\circ})$, $(75.1\text{--}77.6^{\circ})$, $(77.6\text{--}80.7^{\circ})$, $(80.7\text{--}84.3^{\circ})$, $(84.3\text{--}86.0^{\circ})$.

In the subsequent calculations it was assumed $\Sigma_{\text{P}} = \Sigma_{\text{H}}$ over all high latitudes in summer.

4.2. Space-time distribution of the field-aligned currents $j_{\parallel}(H_{01})$ (summer season)

Figure 13 shows the space-time distribution of the density of the field-aligned current related to the presence of geomagnetic field variations independent of the I.M.F.

The vertical currents $j_{\parallel}(H_{01})$ independent of the I.M.F. occupy the whole high latitude region and were separated into two parts by the meridian 22 h–11 h M.L.T. In the night–pre-noon sector, the current flows into the ionosphere at latitude $70^{\circ} \leq \Phi \leq 85^{\circ}$ and flows out at latitude $60^{\circ} \leq \Phi \leq 70^{\circ}$. In the afternoon–evening, the current flows into the ionosphere at latitudes $60^{\circ} \lesssim \Phi \lesssim 71^{\circ}$ and flows out at latitudes $71^{\circ} \lesssim \Phi \lesssim 86^{\circ}$.

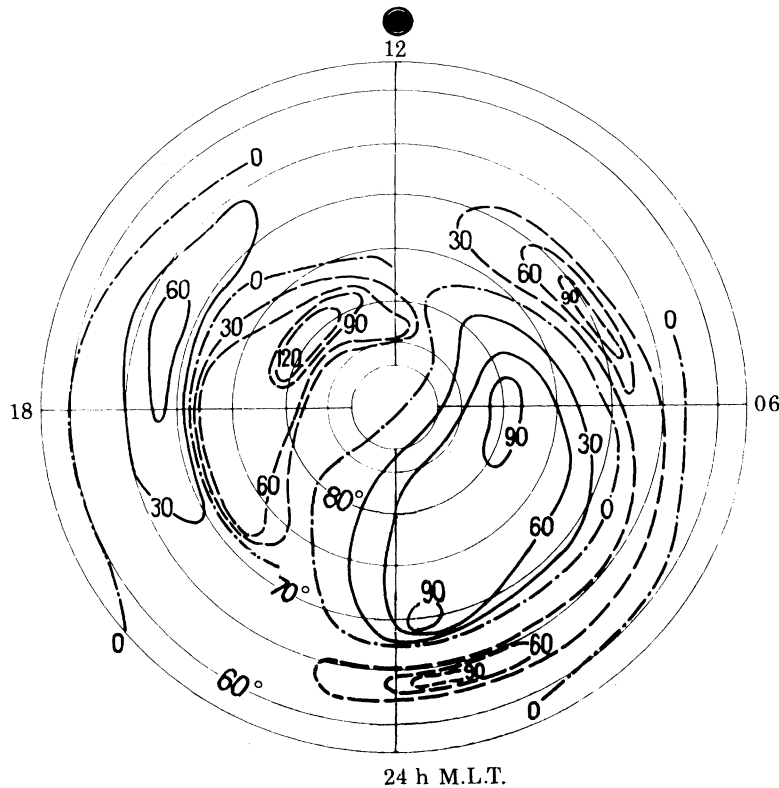


FIGURE 13. Space–time distribution of the field-aligned current $j_{\parallel}(H_{01})$ in the 1968 summer for geomagnetic field variations independent of the I.M.F. and characterized by the term H_{01} in expression (3). Figures on isolines for j_{\parallel} are expressed in mA km^{-2} . Solid lines denote currents flowing into the ionosphere; dashed lines correspond to outward currents. The current distribution corresponds to the following average values of the parameters of solar wind plasma: $\bar{v} = 500 \text{ km s}^{-1}$; $\bar{n} = 4 \text{ cm}^{-3}$. The coordinate system is corrected geomagnetic latitude, local geomagnetic time. In this and subsequent figures isolines enclose regions with field-aligned currents of equal intensity; numbers are in mA km^{-2} .

The field-aligned currents $j_{\parallel}(H_{01})$ have a space–time structure consistent with the large-scale structure of the field-aligned currents observed by the TRIAD satellite at an altitude of 800 km (Iijima & Potemra (henceforth referred to as I.P.) 1976*a, b*; Zmuda & Armstrong 1974). The results obtained enable us to understand the cause of the almost continuous existence of the field-aligned currents in zones 1 and 2 (I.P. 1976*a, b*) by considering them in connection with a continuous outflow from the magnetosphere due to the solar wind. In zone 1, both the maximum current density and the total currents are greater than in zone 2. The methods of TRIAD data selection used did not allow currents to register at an arbitrary level of magnetic disturbances. The weaker currents of zone 2 at $K_p \approx 0$ could not be registered. Moreover, the region in which the field-aligned currents were present, shown in figure 13, occupies the whole of the polar cap at $\Phi > 80^{\circ}$ (Levitin *et al.* 1977), instead of the latitudes of the auroral oval only as was reported by I.P. (1976*a*).

The presence of the field-aligned currents in the whole near-pole region, which was first found from ground-based data by Levitin *et al.* (1977), was confirmed by TRIAD measurements (Saflekos *et al.* 1978).

4.3. Space-time distribution of the field-aligned currents $j_{\parallel}(K^{B_z < 0})$

The field-aligned currents controlled by the southward I.M.F. component ($B_z < 0$) for a variation in B_z of -1 nT are shown in figure 14. The currents occupy the whole high latitude region and divide it, depending on their direction, into two regions with a boundary along the 11 h–21 h M.L.T. meridian.

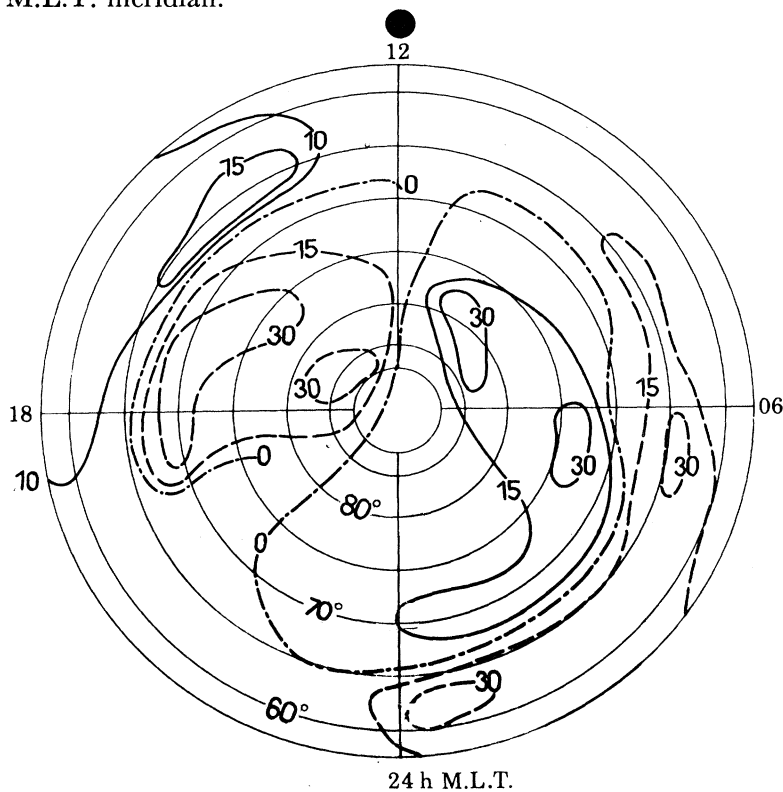


FIGURE 14. Space-time distribution of the field-aligned currents $j_{\parallel}(K^{B_z < 0})$ controlled by the southward I.M.F. component ($B_z < 0$) for a variation B_z by -1 nT for the 1968 summer.

In the sector 21 h–11 h M.L.T., the current flows into the ionosphere at latitudes $68^{\circ} \leq \Phi \leq 86^{\circ}$ and flows out at latitudes $68^{\circ} \leq \Phi \leq 60^{\circ}$. In the afternoon sector, the current flows into the ionosphere at latitudes $60^{\circ} \leq \Phi \leq 68^{\circ}$ (13 h–19 h M.L.T.) and flows out at latitudes $68^{\circ} \leq \Phi \leq 86^{\circ}$ (12 h–19 h M.L.T.).

The space-time structure of the field-aligned currents $j_{\parallel}(K^{B_z < 0})$ (figure 14) is similar to that shown in figure 13 for the currents $j_{\parallel}(H_{01})$ independent of the I.M.F. During periods of enhanced geomagnetic activity ($B_z < 0$), the currents of figures 13 and 14 are added together. Therefore, zones 1 and 2 of the field-aligned currents registered by the TRIAD satellite, according to I.P. (1976*a, b*), are just the total distribution of the field-aligned currents divided into one part that exists for all times and another that is generated only when $B_z < 0$.

From the results of the calculations of the field-aligned currents, one can explain the TRIAD satellite observations as follows. The field-aligned currents are present in the whole region

$\Phi \geq 60^\circ$. A satellite with a sufficiently sensitive magnetometer can register the currents in spite of their small amplitude. With the method of experimental data selection described, however, the currents are assumed to exist only if their amplitude is greater than $0.25 \times 10^{-6} \text{ A m}^{-2}$. As a result, in the absence of noticeable geomagnetic disturbances, $AL \leq 100 \text{ nT}$, a satellite registers the field-aligned currents when passing the region of the maximum field-aligned currents shown in figure 13. During geomagnetic disturbances ($B_z < 0$) the field-aligned currents are registered when the satellite crosses the region where the total field-aligned current distribution is at a maximum.

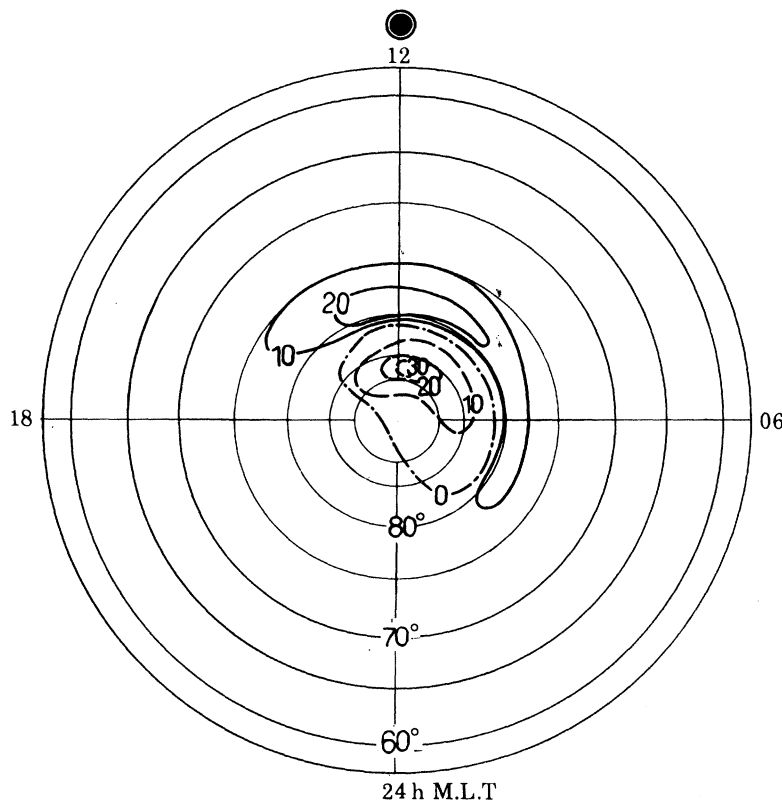


FIGURE 15. Space-time distribution of the field-aligned currents $j_{\parallel}(K^{B_y > 0})$ controlled by B_y for a variation in B_y of $+1 \text{ nT}$ for the 1968 summer for $B_z > 0$. (For a variation in B_y of -1 nT , the field-aligned currents will be in the opposite direction.)

4.4. Space-time distribution of the field-aligned currents $j_{\parallel}(K^{B_y > 0})$

In figure 15 is presented the space-time distribution of the field-aligned currents $j_{\parallel}(K^{B_y > 0})$ controlled by B_y for a variation in B_y of 1 nT , for $B_z > 0$. The direction of the field-aligned currents will be reversed with a variation in B_y of -1 nT .

The field-aligned current controlled by B_y flows into the ionosphere at latitudes $76^\circ \leq \Phi \leq 80^\circ$ in the sector 03 h–16 h M.L.T. and flows out for latitudes $\Phi \gtrsim 80^\circ$ in the sector 02 h–15 h M.L.T. This large-scale distribution of the field-aligned currents is similar to that obtained by Fairmark *et al.* (1976).

For $B_z < 0$, the field-aligned currents controlled by B_y are shifted to lower latitudes than for $B_z > 0$, with a simultaneous increase in the area covered by the currents. The field-aligned currents $j_{\parallel}(K^{B_y > 0})$ are concentrated mainly in the day-cusp region and in the polar cap. When combined with currents due to other sources, the field-aligned currents $j_{\parallel}(K^{B_y > 0})$ may either

intensify or weaken the resultant current depending on the direction of B_y . The distribution of field-aligned currents $j_{\parallel}(K^{B_y>0})$ presented in figure 15 is in good agreement with the model of Lyatsky (1978) and Volland (1973). This distribution was, however, apparently first obtained, from ground-based data by Fairmark *et al.* (1976). It is in fair agreement with the results obtained by Wilhelm *et al.* (1978) based on both ground-based observations and satellite data.

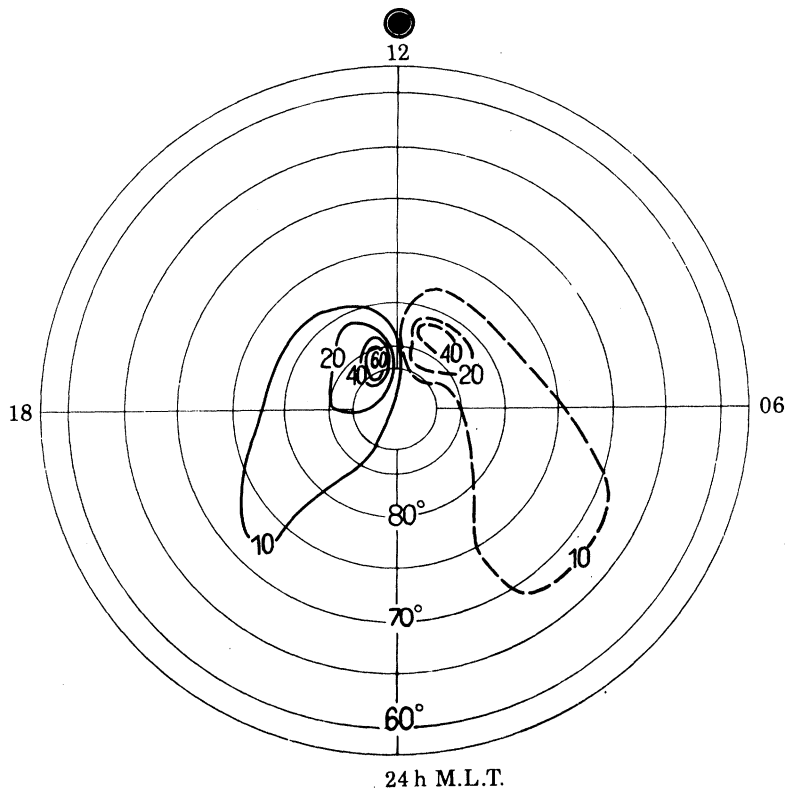


FIGURE 16. Space-time distribution of the field-aligned currents $j_{\parallel}(K^{B_z>0})$ controlled by $B_z > 0$ for a variation in B_z of 1 nT for the 1968 summer.

4.5. Space-time distribution of the field-aligned currents $j_{\parallel}(K^{B_z>0})$

In figure 16, the space-time distribution is presented for the field-aligned currents $j_{\parallel}(K^{B_z>0})$ controlled by $B_z > 0$. The currents are located mainly in the polar cap: the current flows into the ionosphere at latitudes $72^{\circ} \leq \Phi \leq 86^{\circ}$ in the sector 12 h–21 h M.L.T. and flows out at latitudes $68^{\circ} \leq \Phi \leq 86^{\circ}$ in the sector 02 h–12 h M.L.T.

The space-time structure of the maximum field-aligned current dependent on $B_z > 0$ corresponds to the structure of currents registered by the TRIAD satellite in the day-cusp region (zone 3 of I.P. (1976*b*)). Actually, these currents flow into the afternoon sector and out from the pre-noon sector, i.e. the currents are in opposite directions to those usually observed in these time sectors at the latitudes of the auroral oval in zone 1 (see figures 13 and 14). According to I.P. (1976*b*), however, the field-aligned currents in zone 3 are controlled by $B_z < 0$. Although it was noted by Iijima *et al.* (1978) that the currents in zone 3 reach large values both for $B_z < 0$ and for $B_z > 0$, it is still uncertain from satellite observations whether a large-scale distribution exists of the field-aligned currents controlled by $B_z > 0$ and what its configuration would be. The presence of these currents was indicated by observations of the

field-aligned currents for some passes of ISIS-2 and TRIAD (McDiarmid *et al.* 1977; Potemra *et al.* 1979). Some indications were also presented by Nishida (1978) of a possible connection of the field-aligned currents controlled by $B_z > 0$ with zone 3 of the field-aligned currents. When comparing the satellite measurements of field-aligned currents in the cusp region with results obtained from ground-based observations of magnetic field variations, one should, however, bear in mind that a space-time distribution of the field-aligned currents for a given instant is determined by the resultant action of the various I.M.F. components and solar wind parameters. Therefore, the direction of the resultant field-aligned current, even with $B_z > 0$, is not always identical to that in figure 16.

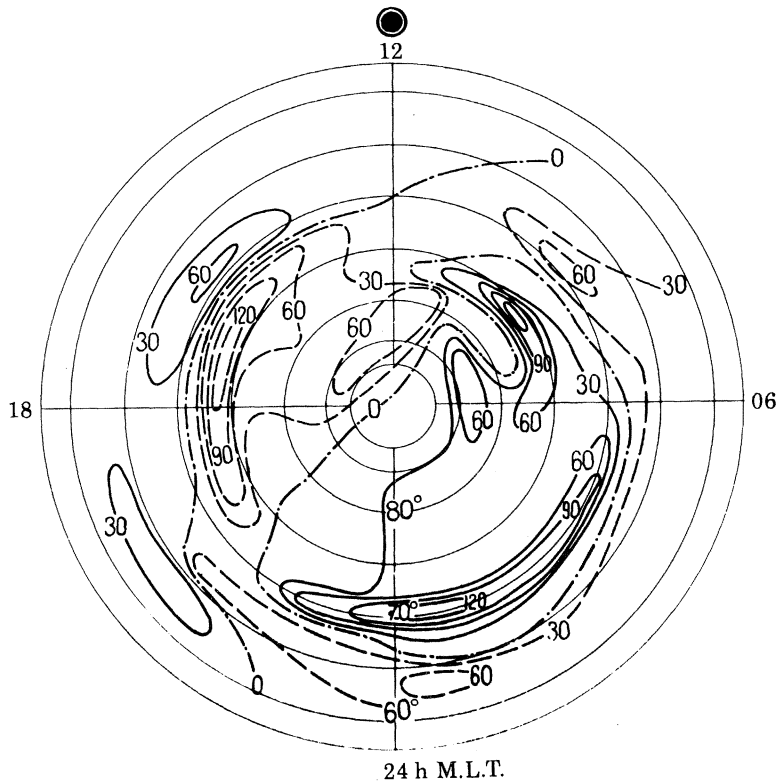


FIGURE 17. Space-time distribution of the field-aligned currents $j_{\parallel}(K^{v^2}\bar{v}^2 + K^{nv^2}\bar{n}\bar{v}^2)$ for the variations connected with the average values of the parameters v^2 and nv^2 of the solar wind for the 1968 summer.

4.6. *Space-time distribution of the field-aligned currents controlled by parameters of the solar wind plasma*

Figure 17 shows the distribution of field-aligned currents $j_{\parallel}(K^{v^2}\bar{v}^2 + K^{nv^2}\bar{n}\bar{v}^2)$ flowing into and out from the ionosphere at high latitudes in the summer for $B_z > 0$. Calculations have been made by using equation (5) for the distribution of the magnetic variations, characterizing their relation to the parameters v^2 and nv^2 for the average values, \bar{v}^2 and $\bar{n}\bar{v}^2$. Thus $j_{\parallel}(K^{v^2}\bar{v}^2 + K^{nv^2}\bar{n}\bar{v}^2)$ in figure 17 characterizes, in a pure form, the distribution of the field-aligned currents controlled by the velocity, density and temperature of the solar wind.

In the morning sector, the currents flow into the ionosphere in the wide range of geomagnetic latitudes $65^\circ \leq \Phi \leq 86^\circ$ in the sector 22 h–11 h M.L.T. The currents flowing out from the ionosphere in the same time sector are located at lower latitudes. It seems that both the ionospheric and field-aligned currents controlled by the solar wind parameters are not restricted

to the region $\Phi > 60^\circ$ but extended equatorwards from this latitude, possibly even to mid-latitudes. If so, variability in the velocity and density of the solar wind should result in day-to-day fluctuations in the S_q -variations of the geomagnetic field at mid-latitudes.

In the evening sector, the currents flow into the ionosphere for $\Phi < 71^\circ$ and flow out at higher latitudes. The distribution of $j_{\parallel}(K^{v^2}\bar{v}^2 + K^{nv^2}\bar{n}\bar{v}^2)$ in figure 17 is similar in its general features to the distribution presented in figure 13. This indicates that field variations independent of the I.M.F. are controlled mainly by the parameters of the solar wind plasma. Differences in topology and amplitudes between figures 13 and 17 result from the fact that figure 13 includes currents controlled by the parameters of the solar wind plasma, currents related to the dynamo-action of the atmospheric winds, currents controlled by $|B_y|$ and currents controlled by other parameters about which insufficient is known at present. The differences between j_{\parallel} in figures 13 and 17 may also be caused, to a certain extent, by the different methods used in choosing a reference level for the field variations.

4.7. A model of the field-aligned currents

We shall present subsequently all the parameters needed to estimate the intensity and direction of the resultant field-aligned current of the I.M.F.-dependent currents and I.M.F.-independent currents in a certain cell on the Φ, t -diagram for $\Phi \geq 60^\circ$, t being the time in M.L.T.

The intensity and direction of the resultant field-aligned current I (A km^{-2}) for each cell are determined from the relation

$$I(\Phi, t) = I_{\pm x}B_x + I_{\pm y}B_y + I_{\pm z}B_z + I_0,$$

where I is the hourly-mean value of a field-aligned current density for the time (U.T.) at which hourly-mean values are known of B_x, B_y, B_z in the solar-ecliptic coordinate system. In this case, $I > 0$ corresponds to the current flowing into the ionosphere, and $I < 0$ to the current flowing out. The plus (minus) sign in the coefficients $I_{\pm x}, I_{\pm y}, I_{\pm z}$ means that the coefficients are used to estimate the currents when $B_z > 0$ (< 0).

The values of the coefficients $I_{\pm x}, I_{\pm y}, I_{\pm z}$ and I_0 at hourly intervals for the following space cells $\Delta\Phi$, ($57.2\text{--}59.8^\circ$), ($59.8\text{--}62.5^\circ$), ($62.5\text{--}64.9^\circ$), ($64.9\text{--}68.2^\circ$), ($68.2\text{--}71.3^\circ$), ($71.3\text{--}75.1^\circ$), ($75.1\text{--}77.6^\circ$), ($77.6\text{--}80.7^\circ$), ($80.7\text{--}84.3^\circ$), ($84.3\text{--}86.0^\circ$), are presented by Afonina *et al.* (1979*b*) and in our table 3 for the summer season. These data represent the correlation model connecting the field-aligned current density with I.M.F. variations for the year of maximum solar activity (1968). It seems, however, that the model can be extrapolated to the summer of any year, since the amplitudes of j_{\parallel} constructed according to the model have an appreciative character. With hourly-mean I.M.F. and geomagnetic field components obtained from an insufficiently dense network of observatories and with the uniformly conducting ionosphere adopted for the simulations we cannot obtain a sufficiently detailed latitude profile of the field-aligned current for a given instant. This model, however, allows us to make comparisons between the field-aligned currents at various latitudes and longitudes in the region $\Phi \geq 60^\circ$, and its application to the analysis of the satellite data, as will be shown subsequently, enables us to decipher some complicated satellite magnetograms depending on conditions in interplanetary space. The current densities j_{\parallel} , calculated in the model, appear to be lower than the densities presented by I. P. (1976*a, b*).

5. ANALYSIS OF THE FIELD-ALIGNED CURRENT MEASUREMENTS OF THE TRIAD AND ISIS SATELLITES

Using the model presented in §4.7 for the field-aligned currents, we shall attempt to decipher the board magnetograms for certain satellite passes, to detect the parameters of interplanetary space that cause the distribution of j_{\parallel} observed in a given flight.

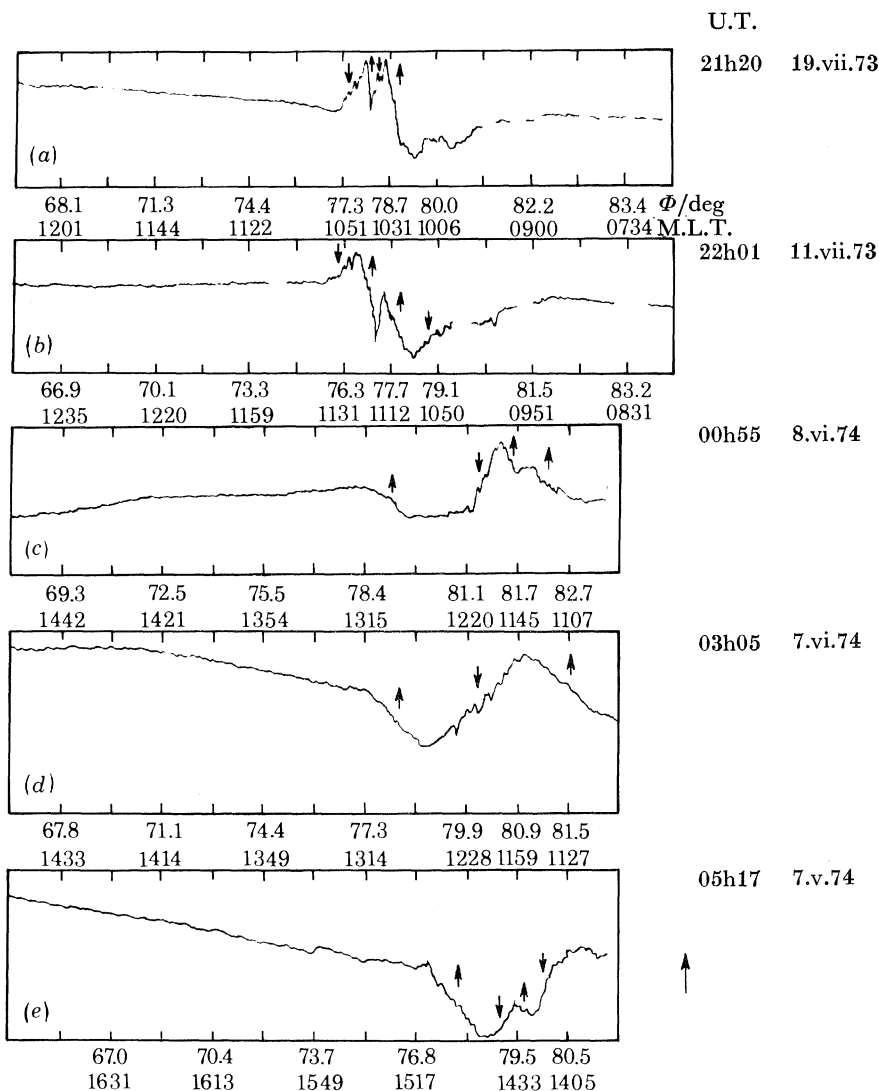


FIGURE 18. Magnetograms from the TRIAD satellite during the summer season (from I.P. 1976 *a, b*). Arrows on the diagrams give the direction of the field-aligned current determined from the character of the fluctuations of the geomagnetic field component in the east-west direction. Parts (a) and (b) are for pre-noon passes; (c), (d) and (e) for afternoon passes. Arrow to the right of (e) represents a field of 500 nT.

5.1. Analysis of TRIAD passes through the day-cusp region

In figure 18 magnetograms from the TRIAD satellite are presented for the summer season (I.P. 1976 *b*), for both pre-noon (figure 18 *a, b*) and afternoon (figure 18 *c-e*) passes. The figure also shows the date of the pass, corrected geomagnetic latitude (Φ) and the direction

of the field-aligned currents determined from the character of the fluctuations of the east–west geomagnetic field component. The passes used were those for which data on the I.M.F. were available (King 1975). These passes provided the basis for the introduction by I.P. (1976*b*) of zone 3 of the field-aligned currents, which is related to the day-cusp region where the field-aligned current flows out from the ionosphere in pre-noon hours and flows in during the afternoon.

Table 4 gives the following data for TRIAD passes through the region of field-aligned currents: hourly-mean values of B_x , B_y and B_z , at the time of a pass, in the solar-ecliptic coordinate system, according to King (1975); the time of the pass (U.T. and M.L.T.); the space cells $\Delta\Phi$ for which the densities of the field-aligned currents were calculated; densities and directions of field-aligned currents I dependent on B_x , B_y and B_z , and of I_0 which is independent of the I.M.F.; and the resultant current density

$$I = I(B_x) + I(B_y) + I(B_z) + I_0$$

for a given space cell $\Delta\Phi$. The densities of the field-aligned currents were determined by using the model given in §4.7 and are expressed in mA km⁻².

The first two passes, on 19 July and 11 July 1973 (figure 18*a, b*), are for pre-noon M.L.T. intervals when, according to the structure of the field-aligned currents (zones 1 and 2) given by I.P. (1976*a*), the currents should flow out from the ionosphere (zone 2) on the southern boundary of the auroral oval, and into the ionosphere on the northern boundary (zone 1). The magnetograms presented show that, in fact, at latitudes $\Phi \approx 77.5^\circ$ (figure 18*a*) and $\Phi \approx 76.5^\circ$ (figure 18*b*), the field-aligned currents were observed flowing into the ionosphere and were identified by I.P. (1976*b*) with the currents of zone 1. At higher latitudes currents were observed flowing both out from the ionosphere at $\Phi \approx 78^\circ$ (figure 18*a*) and $\Phi \approx 77^\circ$ (figure 18*b*), related by I.P. (1976*b*) to the currents of zone 3, and into the ionosphere at $\Phi \approx 81^\circ$. Calculations by means of the model (table 4) enable us to understand the cause of the presence in the magnetograms of a complicated spatial pattern of field-aligned currents at day-cusp latitudes.

According to table 4, B_x and B_y were negative during the two passes considered. The field-aligned current controlled by B_y appeared to be prevailing in the pre-noon sector. On 19 July 1973, $I(B_y)$ was twice $I(B_z)$ and three times I_0 at latitudes $77.6^\circ \leq \Phi \leq 80.7^\circ$. It is just this current $I(B_y)$ that results in the appearance of a magnetic disturbance that was classified by I.P. (1976*b*) as a separate zone 3 in which the field-aligned current flows out from the ionosphere. At $\Phi < 77.5^\circ$, the presence of outward-flowing currents is both observed, and predicted by the model calculations. The narrow zone of inward-flowing currents at $\Phi \approx 77.5^\circ$ in the model calculations appears as a pronounced decrease of outward currents at latitudes $\Phi = 77.6^\circ$ and $\Phi = 80.7^\circ$. We hope that use of the model calculations with space cells of the order of 1° in latitude will enable us to detect the fine structure of the field-aligned currents. The model calculations explain also the presence of the region of inward-flowing currents controlled by B_y for $\Phi > 80^\circ$. These can be seen in figure 18*a*.

During the pass on 11 July 1973 (figure 18*b*), the conditions in the I.M.F. were similar to those on 19 July except that $|B_y|/|B_z| = 1.4$. The current $I(B_y)$ was again directed from the ionosphere at latitudes $77.6^\circ \leq \Phi \leq 80.7^\circ$, whereas $I(B_z)$ was in the opposite direction. For $\Phi > 80^\circ$, $I(B_y)$ and $I(B_z)$ were flowing into the ionosphere.

Thus the model calculations imply that the direction of a field-aligned current at day-cusp

TABLE 4. DENSITIES OF FIELD-ALIGNED CURRENTS CALCULATED IN THE DEVELOPED MODEL FOR CERTAIN PASSES OF THE TRIAD SATELLITE

date of pass	B_x nT	B_y nT	B_z nT	U.T.	M.L.T. h	$\Delta\phi$ deg.	$I(B_x)$ mA km ⁻³	$I(B_y)$ mA km ⁻³	$I(B_z)$ mA km ⁻³	I_0 mA km ⁻³	ΣI mA km ⁻³
19 July 1973	-0.1	-3.3	-0.8	21h20	11-12	71.3-75.1	0	-16	-4	-20	-40
					10-12	74.1-77.6	0	-66	-2	-10	-78
					10-11	77.6-80.7	0	-50	24	15	-11
					09-10	80.7-84.3	0	50	12	5	67
11 July 1973	-0.9	-3.8	-2.8	22h01	11-12	71.3-75.1	0	-19	-14	-20	-53
					11-12	75.1-77.6	0	-95	-28	0	-123
					10-12	77.6-80.7	-5	-57	42	-2	-22
					08-10	80.7-84.3	0	57	61	12	130
8 June 1974	-2.5	1.8	0.1	00h55	14-15	71.3-75.1	0	0	0	5	5
					13-14	75.1-77.6	0	18	0	-20	-2
					13-14	77.6-80.7	12	36	0	-90	-42
					12-13	80.7-84.3	12	27	0	-60	-21
7 June 1974	-1.8	3.7	1.8	03h05	13-14	71.3-75.1	0	19	0	5	24
					13-14	75.1-77.6	0	37	-36	-20	-19
					12-13	77.6-80.7	0	72	0	-40	32
					11-12	80.7-84.3	9	-37	-18	-60	-106
7 May 1974	-4.0	7.0	4.7	05h17	15-16	71.3-75.1	0	0	47	-20	27
					15-16	75.1-77.6	-20	105	-94	-10	-19
					14-15	77.6-80.7	0	105	23	-120	8
					13-14	80.7-84.3	0	0	165	-60	105

latitudes is determined by B_y and B_z . The interrelation of signs and intensities of B_y and B_z are decisive. The current flowing out from the ionosphere for $77.6^\circ \lesssim \Phi \lesssim 80.7^\circ$ in the pre-noon sector (zone 3) is controlled in the cases considered not by $B_z < 0$, as was assumed by I.P. (1976*b*), but by B_y . It may be possible to explain the inward currents registered on the magnetograms for $\Phi > 80^\circ$ in the framework of the model. The current located polewards from zone 3 was presented by I.P. (1976*b*). From the close relation between the field-aligned currents and the I.M.F. components, it appears that the analysis of TRIAD j_{\parallel} measurements must be made in connection with the I.M.F. conditions ($B_y > 0, B_z > 0$), ($B_y > 0, B_z < 0$), ($B_y < 0, B_z > 0$), ($B_y < 0, B_z < 0$) and the ratio of B_y and B_z , instead of with the level of geomagnetic activity.

The three passes (8 June, 7 June, 7 May 1974) in figure 18*c-e* correspond to the afternoon sector. According to the structure of j_{\parallel} given by I.P. (1976*b*) a field-aligned current flowing out from the ionosphere must be observed in this sector on the poleward side of the auroral oval (zone 1). An outward-flowing current is observed during the satellite passes under consideration at $\Phi \approx 78^\circ$, and according to the model such a resultant current is produced at latitudes $77.6^\circ \lesssim \Phi \lesssim 80.7^\circ$ on 8 June and at $75.1^\circ \lesssim \Phi \lesssim 77.6^\circ$ on 7 June and 7 May (table 4). A current is observed, poleward from the outward current, flowing into the ionosphere. It was identified by I.P. (1976*b*) with zone 3. The model calculations indicated that this current is controlled by B_y , causing the inflow of the resultant current for $77.6^\circ \lesssim \Phi \lesssim 80.7^\circ$ on 7 June and 7 May. (On 8 June, the current flowed inwards for only a very small range in latitude and did not appear in the calculations.) The model calculations are in good agreement with observation for $80.7^\circ \leq \Phi \leq 84.3^\circ$ and give a resultant current outward on 7 and 8 June, but inward on 7 May. The field-aligned currents j_{\parallel} in zone 3 (I.P. 1976*b*) during these passes are also connected, according to the model, mainly with B_y . The current flowing out from the ionosphere in the near-pole region may be very strong for $B_z > 0$ (the pass on 7 May).

Thus the proposed model enables us to determine the very complicated structure of the field-aligned current distribution in the day-time high latitude sector. It is, apparently, not necessary to consider a separate zone 3 connected with the day-cusp region only. Some variants of distributions of the field-aligned currents may be observed in the day-cusp region besides those, presented by I.P. (1976*b*), depending on the interrelation of the values and signs of the I.M.F. components. Moreover, the currents at the day-cusp latitudes are controlled to a considerable extent, by B_y (see McDiarmid *et al.* 1979), and not by $B_z < 0$ as was assumed by I.P. (1976*b*). Figure 18*a-d* shows the presence of field-aligned currents at latitudes higher than those of zone 3. Currents not reflected in the pattern proposed by I.P. (1976*b*) give additional evidence for the need to refine current concepts of the distribution of field-aligned currents and the mechanisms of their origin. Mozer *et al.* (1980) found outward currents in the morning sector poleward from zone 1 for 30% of S3-3 satellite passes and emphasized that such a refinement is necessary.

5.2. Analysis of TRIAD satellite passes crossing the auroral oval

In figures 19 and 20 TRIAD magnetograms are presented for disturbances resulting from field-aligned currents in zones 1 and 2 (I.P. 1976*a, b*; 1978). Table 5, which is similar in form to table 4, presents model calculations for j_{\parallel} for TRIAD passes at the time of which the density of field-aligned currents had been measured. The resulting variations in the geomagnetic field are described in figures 19 and 20.

TABLE 5. DENSITIES OF FIELD-ALIGNED CURRENTS CALCULATED IN THE DEVELOPED MODEL FOR CERTAIN PASSES OF THE TRIAD SATELLITE

date of pass	$\frac{B_x}{nT}$	$\frac{B_y}{nT}$	$\frac{B_z}{nT}$	U.T.	M.L.T. h	ϕ deg.	$\frac{I(B_x)}{\text{mA km}^{-2}}$	$\frac{I(B_y)}{\text{mA km}^{-2}}$	$\frac{I(B_z)}{\text{mA km}^{-2}}$	$\frac{I_0}{\text{mA km}^{-2}}$	$\frac{\Sigma I}{\text{mA km}^{-2}}$
29 April 1974	4.0	-3.5	0.5	06h00	16-17	64.9-68.0 68.0-71.3 71.3-75.1	0 0 0	0 -18 0	0 -3 8	50 30 -60	50 9 -52
22 April 1974	2.4	-3.8	-1.6	06h10	17-18	64.9-68.0 68.0-71.3 71.3-75.1	0 0 -12	-19 -38 19	0 -50 -32	45 50 -70	26 -38 -95
23 May 1974	4.8	-3.6	-2.6	13h46	03-04	59.8-62.5 62.5-64.9 64.9-68.0 68.0-71.3	0 0 0 0	18 0 -36 -36	0 -13 -39 -39	-15 -40 -10 45	-10 -79 -75 114
30 April 1974	6.0	0.7	-3.1	16h56	04-05	59.8-62.5 62.5-64.9 64.9-68.0 68.0-71.3	0 30 0 0	-4 0 4 7	-62 -62 -93 78	0 -30 -10 45	-66 -62 -99 130
15 May 1974	3.2	-3.0	-1.5	02h04	15-16	62.5-64.9 64.9-68.0 68.0-71.3 71.3-75.1	0 -16 16 0	0 0 -45 0	8 22 -37 -52	20 35 20 -20	28 41 -46 -72
25 May 1974	-1.1	-5.5	0.1	02h57	14-15	68.0-71.3 71.3-75.1 75.1-77.6	0 0 5	-28 0 -28	0 0 0	15 5 -60	-13 5 -83
21 June 1974	4.3	-0.1	0.6	01h05	12-13	71.3-75.1 75.1-77.6 77.6-80.7	0 0 0	0 -1 -2	0 -6 0	0 -5 -40	0 -12 -42
18 June 1974	2.1	-4.0	-0.8	00h56	13-14	68.0-71.3 71.3-75.1 75.1-77.6	0 0 31	-20 -40 -80	-8 -12 -12	0 5 -20	-28 -47 -81
16 May 1974	3.7	-7.4	1.0	04h07	14-16	71.3-75.1 75.1-77.6	0 0	0 -74	8 -10	-20 -35	-12 -119
20 June 1974	7.3	-3.8	5.0	01h36	12-13	68.0-71.3 71.3-75.1 75.1-77.6 77.6-80.7 80.7-84.3	0 0 0 0 -36	0 0 -38 -76 0	0 0 -50 0 75	0 0 -5 -40 -60	0 0 -93 -116 -21

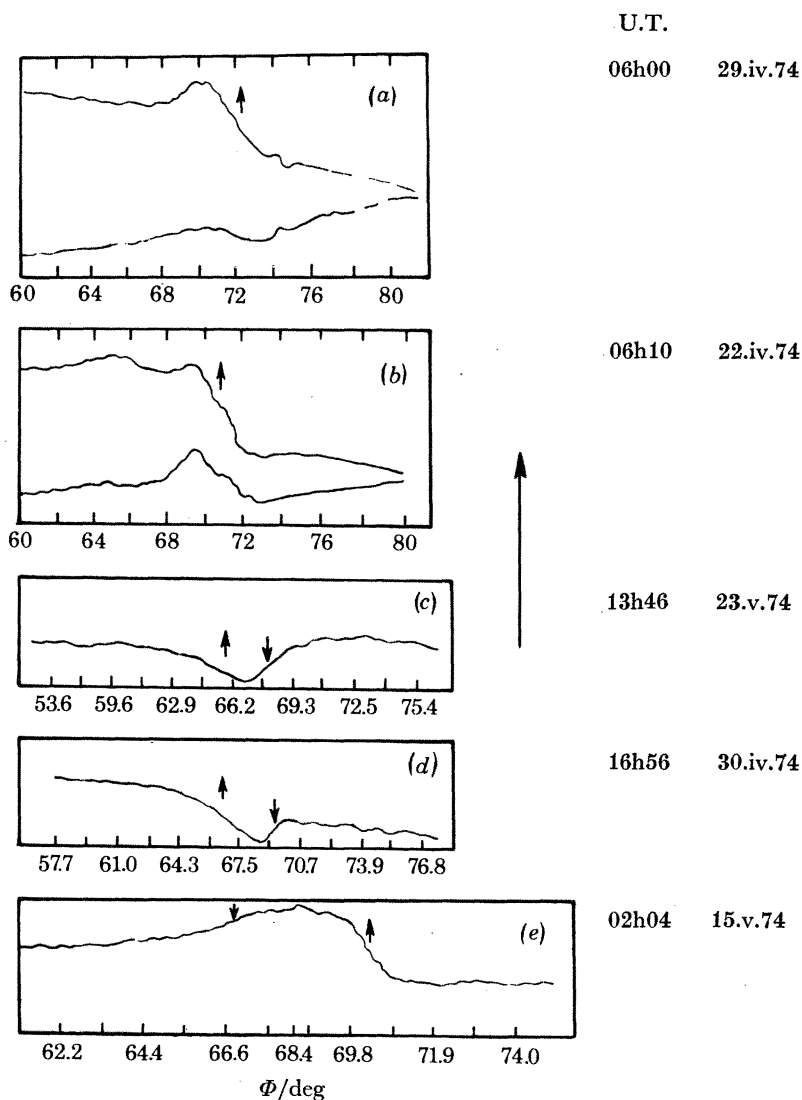


FIGURE 19. Magnetograms from the TRIAD satellite for the disturbances caused by the field-aligned currents of zones 1 and 2 (from I.P. (1976*a, b*; 1978) for various satellite passes. Arrow represents a field to the east.

The pass on 29 April 1974 (06h00 U.T.; 16–17 h M.L.T., figure 19a)

According to the model calculations, the satellite registered mainly the field-aligned currents independent of the I.M.F. These currents gave a resultant flowing into the ionosphere in the southern part of the auroral oval, $\Phi < 71^\circ$, and flowing out in the northern part, $71.3^\circ \leq \Phi \leq 75.1^\circ$. This pass illustrates that the large-scale distribution of the field-aligned currents connected with zones 1 and 2 by I.P. (1976*a, b*; 1978) can be related to field variations due to sources independent of the I.M.F. when the absolute value B_z is small.

The pass on 22 April 1974 (06h10 U.T.; 16–17 h M.L.T.; figure 19b)

The most characteristic feature is the field-aligned current flowing out from the ionosphere at latitudes $69^\circ \leq \Phi \leq 73^\circ$. According to the model calculations, the resultant current j_{\parallel} is

due to currents $I(B_y)$ and $I(B_z)$ at latitudes $68^\circ \leq \Phi \leq 71.3^\circ$, and due to currents $I(B_z)$ and I_0 at latitudes $71.3^\circ \leq \Phi \leq 75.1^\circ$. This pass shows again how strongly dependent on the I.M.F. is the large-scale distribution of field-aligned currents. In different regions of space (Φ, t), the summands of the resultant current occur in different proportions and with different signs resulting in the complicated magnetograms obtained by satellites.

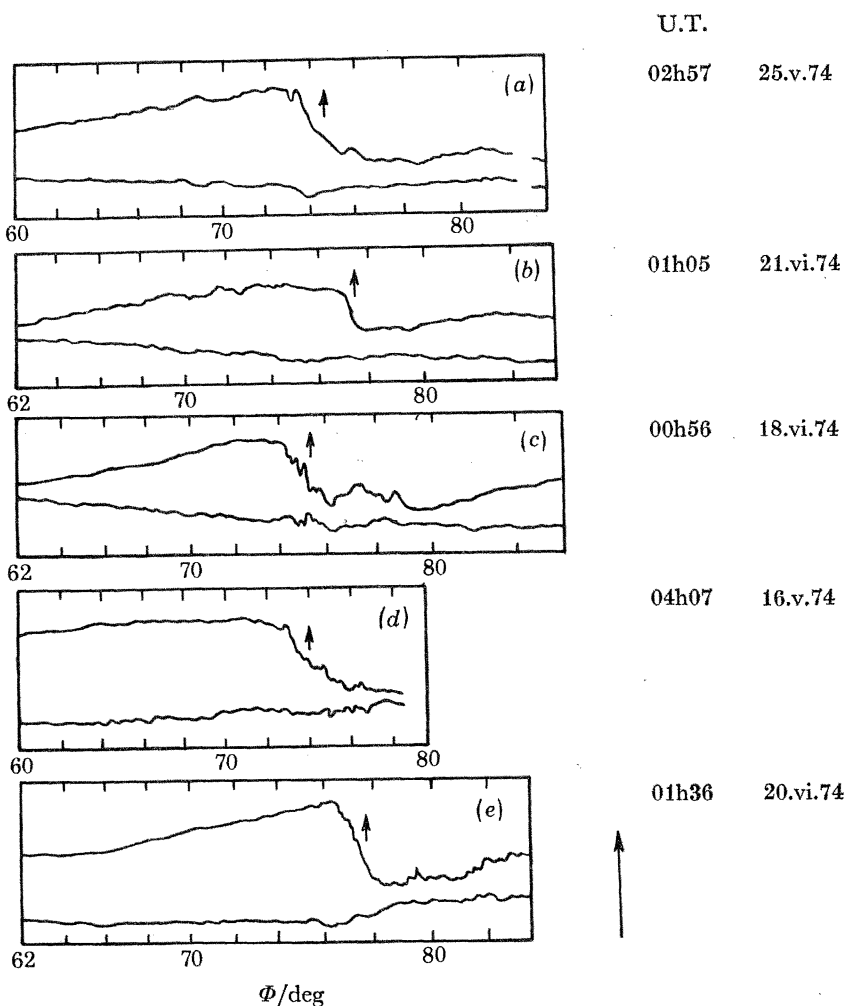


FIGURE 20. As for figure 19. Arrow to the right of (e) represents a field of $1 \mu\text{T}$.

The pass on 23 May 1974 (13h46 U.T., 03–04 h M.L.T.; figure 19c)

On the satellite magnetogram is observed the distribution of field-aligned currents typical of the large-scale zones 1 and 2 in the morning sector (I.P. 1976*a, b*; 1978): on the equatorward side of a disturbance region, the current flows out from ionosphere; on the poleward side the current flows in. The results of the model calculations are in good agreement with observations and indicate that the currents registered in this pass are the result of summing currents controlled by the southward ($B_z < 0$) I.M.F. component, and currents independent of the I.M.F. Some contribution to the resultant distribution of field-aligned currents is given by $I(B_y)$. This fact demonstrates again a close connection between magnetic disturbances and the

conditions in the I.M.F. for certain passes of a satellite. According to the model calculations (table 5) an analogous interpretation can be used for the passes on 30 April 1974 (16h56 U.T.; 04–05 h M.L.T.; figure 19*d*) and on 15 May 1973 (02h04 U.T., 15–16 h M.L.T.; figure 19*e*) (Afonina *et al.* 1979*b*).

The pass on 25 May 1974 (02h57 U.T.; 14–15 h M.L.T.; figure 20a)

During this pass B_z was small. The results of model calculations are in good agreement with observation. According to the calculations, I_0 is itself sufficient to provide a field-aligned current flowing out from the ionosphere at $74^\circ \leq \Phi \leq 76^\circ$. The contribution of $I(B_y)$ (although $B_y = -5.5$ nT) is small compared with that of I_0 . This pass shows again that the effects of the I.M.F. components and of I_0 are different in different parts of the high latitude region.

The pass on 18 June 1974 (00h56 U.T.; 13–14 h M.L.T.; figure 20c)

This pass shows that B_y should play a decisive role in the formation of the resultant field-aligned current flowing out from the ionosphere in zone 1 in the evening sector (as well as in zone 3). In this case, according to model calculations, if B_y were of opposite sign during this pass, the field-aligned current would be in the opposite direction. This result indicates again that it is necessary to classify the passes of the TRIAD satellite in connection with I.M.F. conditions instead of with geomagnetic activity. The interpretation of the data of this pass points to difficulties arising in identifying zones 1 or 3 and, possibly, to a close connection between the currents in zones 1 and 3 in the day-time sector.

The pass on 20 June 1974 (01h36 U.T.; 12–13 h M.L.T.; figure 20e)

For this pass, as well as for that on 22 April 1974, the characteristic feature was an intense field-aligned current flowing out from the ionosphere for $76^\circ \leq \Phi \leq 78^\circ$. According to the model calculations, this current is caused by a source controlled by B_y and B_z . The pass corresponded to local geomagnetic noon when the effects of field-aligned currents controlled by B_y and B_z were most pronounced. Joint action of the currents $I(B_y)$ and $I(B_z)$, both in the same direction, gave the 'smooth' shape of the magnetogram at the latitudes of the maximum disturbance. At higher latitudes ($77.6^\circ \leq \Phi \leq 84.3^\circ$), the resultant current is directed outward from the ionosphere. The direction of the resultant is determined by $I(B_y)$ and I_0 in the region $77.6^\circ \leq \Phi \leq 80.7^\circ$ and by $I(B_z)$ and I_0 in the region $80.7^\circ \leq \Phi \leq 84.3^\circ$. In this case, the current $I(B_z)$ is directed inwards and has intensity equal to that of I_0 . According to the model calculations (table 5) analogous interpretations can be made for the passes on 21 June 1974 (01h05 U.T.; 14–15 h M.L.T.; figure 20*b*) and 16 May 1974 (04h07 U.T.; 14–16 h M.L.T.; figure 20*d*) (Afonina *et al.* 1979*b*).

The analysis of the data performed for the given passes of the TRIAD satellite in connection with the proposed statistical model of the field-aligned currents controlled by the parameters of the interplanetary plasma and the I.M.F. components was based on all published data (up to 1979) for which data on the I.M.F. components were presented by King (1975). We draw the following conclusions from the results of the present analysis.

(i) A comparison of the large-scale space-time distribution of the field-aligned currents for some passes of the TRIAD satellite in various M.L.T. sectors through the high-latitude region with the model calculations of j_{\parallel} provided evidence of the validity of the proposed relations between the field-aligned currents and the I.M.F. components.

(ii) The model representation of the resultant field-aligned current, as a sum of field-aligned currents controlled by various sources, enables us to interpret the complicated distributions of field-aligned currents registered during passes of the TRIAD satellite as being dependent on conditions in the interplanetary space outside the Earth's magnetosphere.

(iii) Field-aligned currents in the evening and morning sectors of the auroral oval are composed, mainly, of currents from two sources: the current system independent of the I.M.F. but controlled by parameters of solar wind plasma; and the current system controlled by the southward ($B_z < 0$) I.M.F. component.

(iv) It seems that the field-aligned currents in the day-cusp region (zone 3 according to I.P. (1976*b*)) and at the latitudes of the day-time part of the auroral oval (zone 1 according to I.P. (1976*a*)) are determined by the currents from sources related to B_y and $B_z > 0$. It appears to be unnecessary to separate the field-aligned currents into zones 1 and 3 (as was done in I.P. (1976*b*)), since the day-time sector of the auroral oval is, evidently, the day-cusp. Various spatial configurations of inward and outward field-aligned currents may be observed, depending on the conditions in interplanetary space at day-cusp latitudes (covering zones 1 and 3). One of the possible configurations is presented by McDiarmid *et al.* (1979) in their figure 9. The other configurations are presented in figures 18 and 20 for daytime passes.

5.3. Analysis of ISIS-2 passes

Magnetograms of the ISIS-2 satellite were presented by McDiarmid *et al.* (1977) for the sector 04–10 h M.L.T. at high latitudes. The magnetometer registered the presence of field-aligned currents in the opposite direction to that of the space-time distribution of j_{\parallel} , according to the pattern presented by I.P. (1976*a*).

We consider, based on the results of the proposed model of field-aligned currents, the passes of ISIS-2 presented by McDiarmid *et al.* (1977). Table 6, which is similar in form to tables 4 and 5, presents model calculations of j_{\parallel} for passes of ISIS-2.

The pass on 10 March 1972 (01h00 U.T.; 05–09 h M.L.T.)

According to the model, an inward field-aligned current exists at latitudes $75^{\circ} \leq \Phi \leq 80.7^{\circ}$, the main contribution to which is given by $I(B_y)$ and I_0 . At latitudes $80.7^{\circ} \leq \Phi \leq 86^{\circ}$, j_{\parallel} is determined by $I(B_y)$ and $I(B_z)$; the resultant current is directed outward. For this pass, however, the large value of B_y ($B_y = 6$ nT) appears to be the determining factor in the resultant distribution. Therefore, there is additional evidence in favour of the conclusion reached in §5.2 that during satellite passes a large-scale j_{\parallel} -distribution is determined by conditions in the interplanetary space. Sometimes, these conditions result in a j_{\parallel} -distribution in the opposite direction to that usually observed. Moreover, the model j_{\parallel} -calculations have shown that j_{\parallel} being in the opposite direction for a given pass of ISIS-2 was not determined by $B_z > 0$, as was assumed by McDiarmid *et al.* (1977), but by the high intensity of B_y .

The interplanetary space conditions during the pass on 10 March 1972 (03h00 U.T.; 6–10 h M.L.T.) were the same as those during the pass at 01h00 U.T. Therefore a similar distribution of the field-aligned currents was registered by the satellite.

The pass on 27 June 1972 (13h00 U.T.; 07–08 M.L.T.)

According to the model calculations, at latitudes $75^{\circ} \leq \Phi \leq 80^{\circ}$ the resultant current flows into the ionosphere and is determined mainly by I_0 . At higher latitudes, $\Phi > 81^{\circ}$, the current

flows out from the ionosphere. The main contribution to the current is given by $I(B_y)$ and $I(B_z)$. The combination $B_y > 0$, $B_z > 0$ in interplanetary space results in the production of an outward field-aligned current in the given high latitude sector.

The pass on 6 July 1972 (11h00 U.T.; 07–11 h M.L.T.)

During the pass, $B_y = 0$ and the resultant field-aligned current was determined by $I(B_z)$ and I_0 . At latitudes $75^\circ \leq \Phi \leq 80^\circ$, the current I_0 prevails over $I(B_z)$, and the resultant current flows into the ionosphere. At $80.7^\circ \leq \Phi \leq 84.3^\circ$, the opposite occurs: $I(B_z)$ is larger than I_0 and the resultant current is outward. The high intensity of B_z ($B_z = 5$ nT) determines the field-aligned current distribution in this pass.

The pass on 23 June 1973 (90h00 U.T.; 04–05 h M.L.T.)

As in the previous pass, $B_y = 0$. The resultant current is again determined by the relation between $I(B_z)$ and I_0 . For $77.6^\circ \leq \Phi \leq 84.3^\circ$, since $I_0 > I(B_z)$, the field-aligned current is directed inward. For $\Phi > 84.3^\circ$, $I(B_z)$ begins to exceed I_0 . This results in a change of direction in the total outward current $I = I_0 + I(B_z) + I(B_x)$ in this high-latitude region with the given I.M.F. conditions.

Summarizing the analysis of j_{\parallel} -distributions from the data of ISIS-2, which are in the opposite direction to those usually observed in the morning sector, we draw the following conclusions.

(i) Depending on interplanetary space conditions, j_{\parallel} -distributions can be observed in the opposite direction to the usual distributions.

(ii) The 'inverse' distributions are not always caused by $B_z > 0$. Sometimes, a substantial contribution is caused by the azimuthal (B_y) component;

(iii) The proposed model, connecting a large-scale j_{\parallel} -distribution with the conditions in interplanetary space, can explain the great variety of j_{\parallel} -distributions observed by satellites.

6. DISCUSSION

1. The above analysis has shown that geomagnetic variations in the high-latitude region $\Phi \geq 60^\circ$ can be represented in the form of a sum of 'elementary' three-dimensional current systems. The summands are: (a) the current systems controlled by B_y (its symmetric and asymmetric components); (b) the current systems controlled by B_z (for $B_z < 0$ the current in the polar cap is directed towards the sun, and for $B_z > 0$ it is directed away from the sun); (c) current systems independent of the I.M.F. (they are similar to those related to $B_z < 0$).

Current systems independent of the I.M.F. are controlled by the density and velocity of the solar wind (and, possibly, by a thermal pressure). They can be represented as a sum of current systems, one controlled by $nv^2 \propto nT_p$, the other governed by v^2 . Moreover, at high latitudes, the current system S_q^0 is an extension of the mid-latitude S_q -system.

2. The detected equivalent current systems give a good representation (with an accuracy of *ca.* 30 nT in summer) of the actual geomagnetic variations in the polar cap. At auroral and subauroral latitudes in summer the difference between calculated (according to the proposed model) and observed values of geomagnetic fields is *ca.* 50 nT. During a substorm, as well as in winter, the adequacy of the model worsens considerably. This indicates that a correlation between the hourly-mean values of the geomagnetic field observed on the Earth's surface and

the interplanetary fields detects only the stationary relations between them. When non-stationary phenomena are superimposed on the stationary phenomena (for example, a sudden increase of conductivity in a local ionospheric region or inhomogeneity of ionospheric conductivity in the winter season), the statistical relation becomes unstable. Therefore, further progress in simulating geomagnetic variations is possible only by analyzing correlation relations between more detailed values (for example the mean for each minute) of the field components on the ground and the solar wind parameters, the dynamics of the ionospheric conductivity above the point of observation at that time being included.

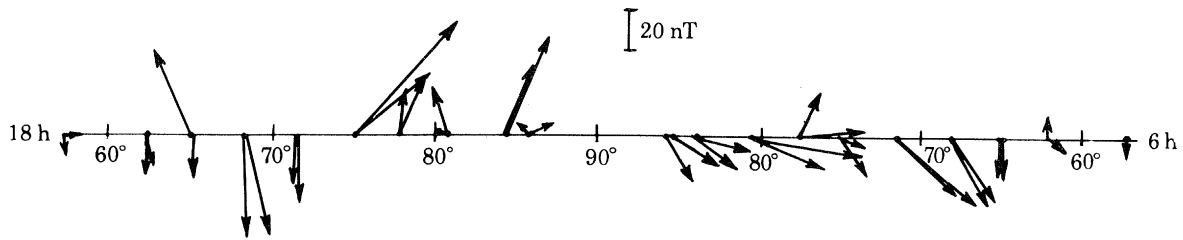


FIGURE 21. Distribution of the vector of equivalent current along the morning-evening meridian, calculated with the following interplanetary medium parameters: $B_z = 4$ nT, $B_y = 0$, $n = 5$ cm $^{-3}$, $v = 400$ km s $^{-1}$.

The proposed model of geomagnetic field variations in connection with the solar wind parameters enables us to understand the conditions in the interplanetary medium, providing a realization of unusual ionospheric current systems considered by Horwitz & Akasofu (1979), Rezhnev *et al.* (1980) and Burke *et al.* (1979). Figure 21 presents a distribution of directions and intensities of the currents along the morning-evening meridian at ten points corresponding to the positions of the magnetic observatories. The vectors of magnetic disturbances were calculated for 05–06 h, 06–07 h, 17–18 h and 18–19 h M.L.T. The calculations were made with the following values for the solar wind parameters: $B_z = 4$ nT, $B_y = 0$, $n = 5$ cm $^{-3}$, $v = 400$ km s $^{-1}$. In the central part of the polar cap, the currents flow antisolarwise within a limited region (the electric field is directed from the evening to the morning side), but the whole distribution of the current arrows corresponds to a four-vortex current system. This system arises in the polar cap as a result of a superposition of the currents controlled by the velocity and density of the solar wind on the currents controlled by $B_z > 0$. The component $B_z > 0$ determines the appearance of the electric field in the polar cap, it being directed from the evening to the morning side. The model presented enables us to understand the causes of the discrepancy between the current systems in the polar cap at $B_z > 0$ presented by Horwitz & Akasofu (1979) and by Maezawa (1976*a*). This discrepancy is not caused by the principle difference, i.e. the different approaches to the geometry of reconnection of the interplanetary and geomagnetic fields (as was assumed by Horwitz & Akasofu (1979)), but by the fact that the current system in Maezawa (1976*a*) reflects the effect of $B_z > 0$ only, whereas in Horwitz & Akasofu (1979) the current system is controlled by the solar wind plasma as well as by $B_z > 0$.

3. The obtained correlations between geomagnetic field variations on the ground and the I.M.F. components enable us to estimate B_y and B_z in summers of maximum solar activity from ground-based geomagnetic data, by using the methods described. With a network of stations, separated by a latitude step $\Delta\Phi = 1^\circ$ on several meridians in the northern and

southern polar caps, continuous estimation would be possible throughout the year for all I.M.F. components, with an accuracy ± 1 nT. In figure 22 the curves of calculated hourly-mean values of (a) B_y and (b) B_z as presented for 6–10 May 1968. The period was selected so that direct measurements of the I.M.F. components were available at the beginning and end of the period, while in the middle data of this kind were absent (King 1975). Good agreement between calculated and observed hourly field values enables us to recommend the methods developed of filling the gaps in the King (1975) catalogue.

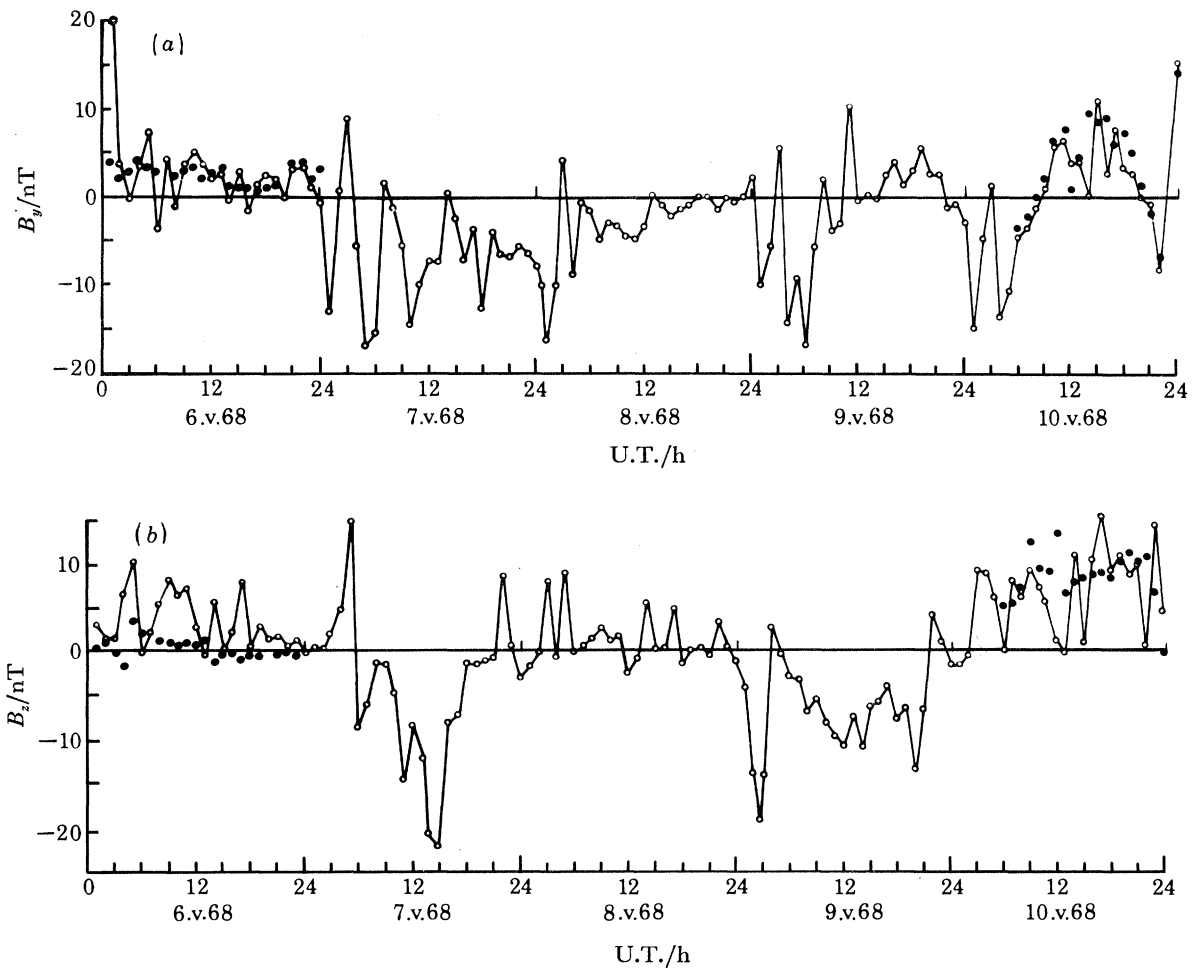


FIGURE 22. Observed (●) and calculated (○) values of (a) B_y and (b) B_z for the period 6–10 May 1968.

4. The distributions of field-aligned currents reconstructed from the data of ground-based observations of the variations of geomagnetic field by means of the relation $j_{\parallel} \approx \text{div } H$, make it possible to understand the statistical space–time pattern of such currents presented by I.P. (1976*b*) and McDiarmid *et al.* (1979). The assumptions made in j_{\parallel} -calculations can be proved as follows.

(a) The current j_{\parallel} is assumed to be normal to the ionosphere. Actually, the field-aligned currents, coincident with the direction of geomagnetic lines of force, are inclined to the ionosphere surface at the angle $\mathcal{H} < 90^{\circ}$. However, the value $j_{\parallel} \sin \mathcal{H} = j_{\text{calculated}}$ is inconsiderably different from j_{\parallel} everywhere at high latitudes, $\Phi \geq 60^{\circ}$.

TABLE 6. DENSITIES OF FIELD-ALIGNED CURRENTS CALCULATED IN THE DEVELOPED MODEL FOR CERTAIN PASSES OF THE ISIS-2 SATELLITE (Levitin *et al.* 1977)

date of pass	$\frac{B_x}{nT}$	$\frac{B_y}{nT}$	$\frac{B_z}{nT}$	U.T.	M.L.T. h	$\frac{\Delta\Phi}{deg}$	$\frac{I(B_x)}{mA km^{-2}}$	$\frac{I(B_y)}{mA km^{-2}}$	$\frac{I(B_z)}{mA km^{-2}}$	$\frac{I_0}{mA km^{-2}}$	$\frac{\Sigma I}{mA km^{-2}}$			
10 March 1972	-1.5	6.0	1.0	01h00	05-06	57.2-59.8	0	0	0	5	5			
					06-07	59.8-62.5	0	0	0	5	5	-15	-15	
					06-07	62.5-64.9	0	0	0	0	0	10	-40	-30
					06-07	64.9-68.0	0	0	0	0	0	0	-35	-5
					06-07	68.0-71.3	0	30	0	0	0	0	50	80
					06-07	71.3-75.1	5	30	-5	-5	0	0	45	70
					07-08	75.1-77.6	0	30	-5	-5	0	0	40	75
					08-09	77.6-80.7	0	30	5	5	0	0	20	-90
					08-09	80.7-84.3	0	-90	-20	-20	0	0	10	-145
					08-09	84.3-86.0	0	-150	-5	-5	0	0	5	5
10 March 1972	-2.5	6.0	1.0	03h00	06-07	57.2-59.8	0	0	0	5	5			
					06-07	59.8-62.5	0	0	0	5	5	-15	-15	
					06-07	62.5-64.9	0	0	0	0	0	10	-40	-30
					06-07	64.9-68.0	0	0	0	0	0	0	-35	-5
					06-07	68.0-71.3	0	30	0	0	0	0	30	60
					07-08	71.3-75.1	10	30	-10	-10	0	0	25	50
					07-08	75.1-77.6	0	30	-5	-5	0	0	10	155
					08-09	77.6-80.7	0	150	-5	-5	0	0	5	-130
					09-10	80.7-84.3	0	-90	-45	-45	0	0	5	-210
					09-10	84.3-86.0	0	-180	-20	-20	0	0	-10	-210

(b) The ionosphere is considered as a thin shell, characterized by the height-integrated conductivity. This means that field-aligned currents generated in the magnetosphere are closed, mainly, by horizontal currents at the heights of the ionospheric E-layer, and the currents generated in the ionosphere are closed through the magnetosphere. Leontjev & Lyatsky (1980) have considered the possibility part of the currents is closed through the F-layer. The results of calculations showed that field-aligned currents from the E-layer are not completely closed in the ionosphere, as was assumed by Antonova (1979), but flow, to a considerable extent, through the magnetosphere. The results of calculations for the small-scale currents would apparently be, valid for large-scale currents too.

(c) In the calculations based on equation (5), the magnetic fields due to the currents induced in the Earth were taken into account. It was assumed that the field variation observed on the Earth's surface is caused by both external and internal sources. A relation between the intensity of the real currents in the ionosphere and the field variations on the ground was considered by Kamide & Brekke (1975); and Kamide (1979). It was shown that the actual current density should be increased by a factor of, at least, $\frac{8}{3}$ to take into account the inhomogeneous current distribution over a spherical surface and other effects, when an overhead current approximation is used.

The model j_{\parallel} -values obtained in this paper are less than those presented by I.P. (1976*a*, *b*, 1978). This can, apparently, be explained by the following: first, according to I.P. (1976*a*, *b*), only those satellite passes when $j_{\parallel} \gtrsim 0.25 \text{ A km}^{-2}$ were selected for analysis; secondly, the present model characterizes the hourly-mean j_{\parallel} -values whereas I.P. (1976*a*, *b*) presented statistics for instantaneous values of the field-aligned currents; thirdly, the present model is obtained from geomagnetic data of a less dense network of stations, the average $\Delta\Phi$ between neighbouring stations being 2–2.5°.

5. The space-time distribution of the field-aligned currents above the ionosphere was generalized in the models, based on the observations of the TRIAD satellite given by I.P. (1976*b*) and of ISIS-2 given by McDiarmid *et al.* (1979).

According to I.P. (1976*b*), Iijima *et al.* (1978), there are three zones of field-aligned currents. The currents flow into the ionosphere in the morning and flow out in the evening in zone 1, located on the poleward side of auroral oval. The current direction is reversed in zone 2, located on the equatorial side of the oval. In zone 3, located in the day sector poleward from zone 1 at day-cusp latitudes, the current flows into the ionosphere in the afternoon and flows out in the pre-noon sector. In zone 3, the j_{\parallel} -intensity increases with intensification of the southward ($B_z < 0$) I.M.F. component, and the longitudinal extension of field-aligned currents and the position of the separatrix between the inward and outward currents is determined by B_y . No close correlation was revealed between j_{\parallel} -intensity and B_y in zones 1 and 3.

According to McDiarmid *et al.* (1979), in the morning and evening sectors, magnetic field disturbances can be described by a two-sheet model of the field-aligned currents flowing into the ionosphere and then flowing out of it along the auroral oval. This is similar to the models proposed by I.P. (1976*b*). In the morning sector, however, cases of abnormal (reverse) direction were observed, parallel with the usual direction of the field-aligned currents, flowing into the ionosphere in zone 1 and flowing out from it in zone 2. The intensity of the field-aligned currents in the evening and morning sectors is closely connected with the intensity of B_z .

In the day-time sector (10–15 h M.L.T.), the vector of magnetic disturbance is eastward or westward, depending on the polarity of B_y . In the Northern Hemisphere the disturbance

vector is directed to the east (west) at $B_y > 0$ ($B_y < 0$) and, therefore, the near-pole field-aligned current flows out of the ionosphere for $B_y > 0$ and flows into the ionosphere for $B_y < 0$. The coefficients of correlation between the intensity of a disturbance vector ΔB and the values of B_y and B_z are $r = 0.75$ and $r = 0.58$, respectively.

It is evident that the space–time diagrams of the field-aligned currents according to I.P. (1976*b*), Iijima *et al.* (1978) and McDiarmid *et al.* (1979) are very different. The difference consists of:

(i) According to I.P. (1976*b*) and Iijima *et al.* (1978), the currents in zone 3 both in the Northern and Southern Hemispheres are inward in the afternoon and outward in pre-noon hours independent of the orientation of B_y . According to McDiarmid *et al.* (1979) the field-aligned current of the same direction is inward or outward over the whole day-time sector, dependent on the direction of B_y .

(ii) According to I.P. (1976*b*) and Iijima *et al.* (1978), the j_{\parallel} -intensity in the day-time sector is controlled by $B_z < 0$, but according to McDiarmid *et al.* (1979), the effect of B_y prevails.

The model distributions of the field-aligned currents given by I.P. (1976*b*) and Iijima *et al.* (1978), and by McDiarmid *et al.* (1979), seem to characterize two different approaches. In one, the field-aligned currents in the cusp form a separated zone 3, whereas in the other, the displacement of the morning and evening branches of zones 1 and 2 of the field-aligned currents over latitude and longitude is dependent on sign of B_y (Fujii & Iijima 1979). Fujii & Iijima (1979) have noted correctly that the authors I.P. (1976*b*), Iijima *et al.* (1978) and McDiarmid *et al.* (1979) cannot decide, from data currently available, which of the models is in better agreement with the set of observational data. It is possible that a new model might explain more exhaustively the experimental data. Such a model, based on the relation between the field-aligned currents and the conditions in interplanetary space, has been proposed in the present paper (figures 13–17). According to this model the value and direction of j_{\parallel} are functions of the solar wind parameters at a certain point of space at high latitude (Φ) at a given time (t). The situation is realistic since field-aligned currents of different directions can be observed at the same point of space for different conditions in the solar wind. Therefore the satellite observations of the field-aligned currents should be analysed not in their relation to the level of geomagnetic disturbance (K_p and AE indices), but in connection with the conditions in interplanetary space (the I.M.F. components, and the velocity and density of the solar wind).

6. The model proposed in this paper of the field-aligned currents in the form of a superposition of ‘elementary’ currents, each controlled by its ‘own’ parameter of the interplanetary medium, enables us to understand the nature of the resultant magnetic disturbance registered during a given pass of a satellite through the high-latitude region. It is not necessary to introduce zones 1, 2, 3 in the region of the field-aligned currents. The model results in the conclusion that the field-aligned currents are present in the whole high-latitude region ($\Phi > 60^\circ$). In the most probable situations in the Earth’s environment ($|B_y| = 4$ nT, $B_z = 0$ nT, $n = 4$ cm⁻³, $v = 500$ km s⁻¹), over all latitudes (except for the day-time cusp), the field-aligned currents independent of the I.M.F. prevail. Their space–time distribution (figure 13) is in agreement with the structure of the large-scale field-aligned currents observed by the TRIAD and ISIS satellites at altitudes 800–1400 km (zones 1 and 2). In the day-time cusp region (09–15 h M.L.T. $75^\circ \leq \Phi \leq 80^\circ$), the field-aligned currents controlled by B_y : depending on the polarity of B_y at a given time, one of the directions of the field-aligned current is realized (figure 15).

When $B_z < 0$, the system of field-aligned currents $j_{\parallel}(B_z < 0)$ is superimposed on the system of field-aligned currents independent of the I.M.F. As these systems have almost identical structures, an intensification of the field-aligned currents takes place. In the whole high latitude region the intensified current system arises in agreement with the structure of the large-scale currents presented by I.P. (1976*a*). In the day-cusp region, the direction and intensity of the field-aligned current are determined by the interrelation of B_y and $B_z < 0$.

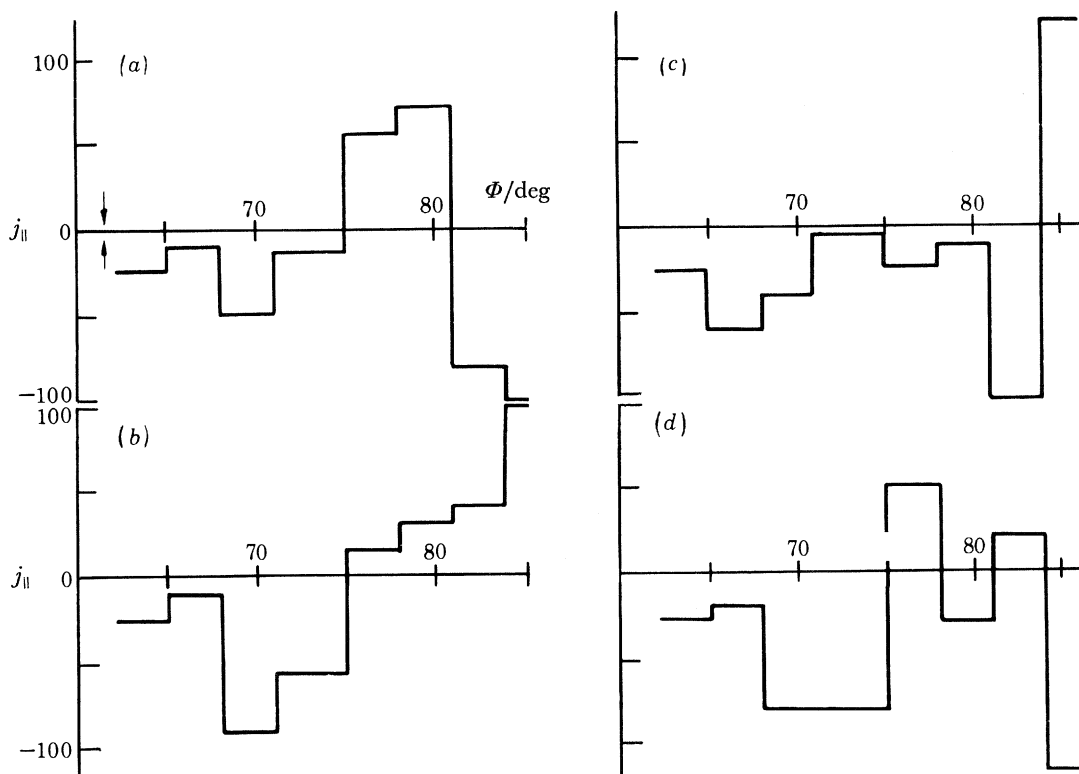


FIGURE 23. Distribution of the field-aligned currents with latitude for 08–09 h M.L.T. and various I.M.F. orientations: (a) $B_y = 4$ nT, $B_z = 2$ nT; (b) $B_y = -4$ nT, $B_z = 2$ nT; (c) $B_y = 4$ nT, $B_z = -2$ nT; (d) $B_y = -4$ nT, $B_z = -2$ nT.

When $B_z > 0$, the system of field-aligned currents independent of the I.M.F. (figure 13) is superimposed on the current system $j_{\parallel}(B_z > 0)$ (figure 16), which is weaker than the former everywhere except in the day-cusp region. The direction and value of the field-aligned currents at latitudes $75^\circ \leq \Phi \leq 85^\circ$ in the 09–15 h M.L.T. sector are determined by a relation between the intensities of B_y and $B_z > 0$. The system of the field-aligned currents $j_{\parallel}(B_z > 0)$ is identical in location and current direction to zone 3 of I.P. (1976*b*).

A limitation on the model proposed by I.P. (1976*b*) and by McDiarmid *et al.* (1979) for the spatial distribution of field-aligned currents was confirmed recently. A statistical analysis of the spatial distribution of the field-aligned currents from the data of the S3–3 satellite given by Mozer *et al.* (1980) and Cattell *et al.* (1979) has shown that in the morning sector from 02–10 h M.L.T., the current flows out from the ionosphere in the equatorward part of the auroral zone and flows inward in the poleward part. The outward current was, however, observed in one-third of the passes to be northward of the current flowing into the ionosphere. The presence

of such a three-sheet current was not implied in the models given by I.P. (1976*b*) and McDiarmid *et al.* (1979).

Let us consider the situations in the interplanetary space when the appearance of three-sheet currents in the required direction is possible, according to the model proposed here for the field-aligned currents. In figure 23, the directions (downward arrow corresponds to inward current, upward arrow corresponds to outward current) and j_{\parallel} -values are presented at various latitudes in the 08–09 h M.L.T. sector for various combinations of B_z and B_y . The total current is presented, including I_0 . It is seen that in late morning for certain combinations of B_z and B_y ($B_z = 2$ nT; $B_y = 4$ nT) a three-sheet structure can arise. In this case, the current flows out for $\Phi < 75^\circ$ in for $75^\circ \leq \Phi \leq 81^\circ$ and flows out again for $\Phi > 81^\circ$. With the assumption that $B_z \geq 0$ and $B_y \geq 0$ are equally probable, the three-sheet structure should be observed in about one quarter of the S3–3 passes.

As noted above, one of the differences between the models proposed by I.P. (1976*b*) and by McDiarmid *et al.* (1979) for the distribution of the field-aligned currents in the day-time sector is as follows. According to McDiarmid *et al.* (1979), the current direction over the whole day-time sector is determined by the polarity of B_y whereas, according to I.P. (1976*b*), at certain hours M.L.T. the current was inward in the afternoon and outward in the morning independent of the polarity of B_y . According to Fujii & Iijima (1979), these intervals can be 10–11 h M.L.T. (outward current) and 13–14 h M.L.T. (inward current).

Using the new model proposed in this paper for the space-time distribution of the field-aligned currents, a calculation was made of the latitude distribution of j_{\parallel} at 10–11 h and 13–14 h M.L.T. for various orientations and values of B_z and B_y . At latitudes $75^\circ \leq \Phi \leq 85^\circ$ the direction and value of j_{\parallel} are substantially dependent on the orientation of B_z and B_y . At 13–14 h M.L.T. at these latitudes, the contribution of I_0 is substantial. Thus the results of the calculations in our model are closer to those obtained by McDiarmid *et al.* (1979), than to those obtained by I.P. (1976*b*), but a substantial contribution of I_0 at some hours masks the effects of the I.M.F.

McDiarmid *et al.* (1980) have presented magnetograms for ISIS-2 passes when $B_z > 0$ was extremely large. In figure 24 the magnetogram given by McDiarmid *et al.* (1980) is presented for the pass on 5 August 1972 at 01h27–01h41 U.T. when the hourly-mean values of the I.M.F. components were $B_z = 30.7$ nT; $B_y = 2.0$ nT; $B_x = -22.2$ nT. The magnetic disturbance was *ca.* 2400 nT in the polar cap for $83^\circ \leq \Phi \leq 84^\circ$ in the day-time sector. It is possible to consider that the experimental data given by McDiarmid *et al.* (1980) finally proved the presence of field-aligned currents controlled by $B_z > 0$ in the day-time sector. The possibility of the presence of these currents and of the ionospheric currents associated with them flowing in an antisolar direction in the polar cap was raised by studies by Maezawa (1976*a*), Levitin *et al.* (1977) and Kuznetsov & Troshichev (1977) but it was, however, considered as doubtful by, for example, Mishin (1979). Friis-Christensen (1979) refers to a paper published by Mishin saying that it shows the presence of a current in the antisolar direction for $B_z > 0$; this is a result of misreading.

Under the magnetogram in figure 24, the densities of the field-aligned currents are presented in mA km⁻² in space-time cells where the satellite occurred. Presented there are contributions of various components controlled by the parameters of the interplanetary medium, and the resultant current ΣI . The model calculations describe the appearance of intense inward and outward currents in the polar cap in the afternoon and morning hours, respectively, although

the model itself was obtained with B_z variations within the limit of several nanoteslas. The high B_z -values in this case determine mainly the intensity and the direction of the resultant field-aligned current.

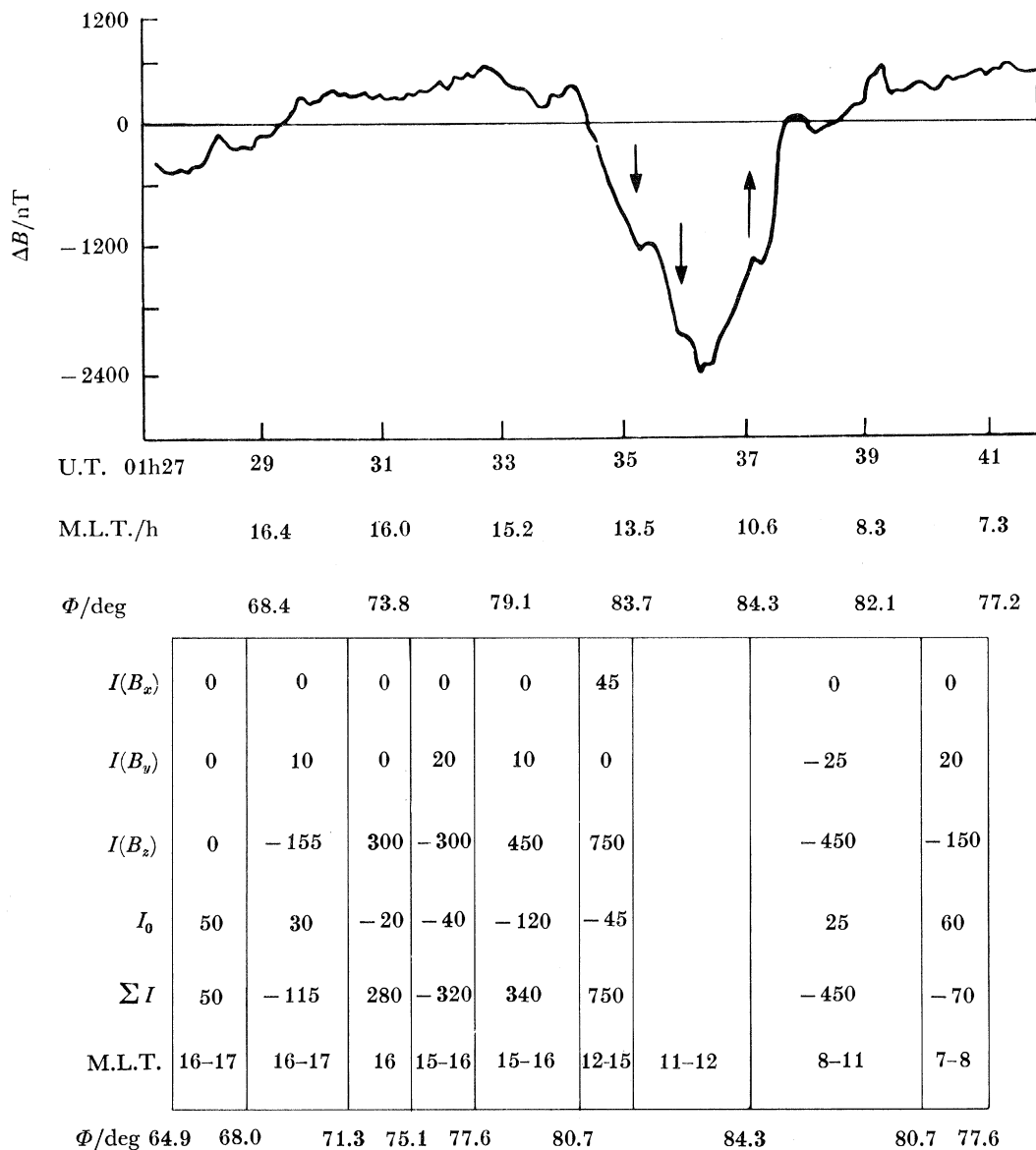


FIGURE 24. Observed and calculated field-aligned currents in the polar cap. The magnetogram is from ISIS-2 satellite observations on 5 August 1972 in the Northern Hemisphere given by McDiarmid *et al.* (1980). Arrows indicate the directions of the field-aligned currents. The table gives values of the field-aligned currents controlled by B_x , B_y and B_z , the value of I_0 , independent of the I.M.F., the resultant current, M.L.T. and Φ ranges near the satellite position.

Hourly values of the I.M.F. components were obtained through NSSDC, WDCA-R and S, hourly values of the geomagnetic field were obtained through WDC B2. We thank B. N. Gassy, Yu. Z. Demidova, T. V. Rodina and V. M. Samohvalova for their contributions to the data processing, calculations and preparation of the paper.

REFERENCES

- Afonina, R. G., Belov, B. A., Levitin, A. E. & Feldstein, Y. I. 1975 In *Interplanetary magnetic fields and geophysical phenomena in high latitudes*, p. 95. Moscow: Nauka.
- Afonina, R. G., Belov, B. A., Levitin, A. E., Markova, M. Yu. & Feldstein, Y. I. 1979a Correlation model of the average hourly values for three components of the geomagnetic field in high latitudes of the north hemisphere (summer 1968, maximum of the solar activity), IZMIRAN preprint no. 10(239), Moscow.
- Afonina, R. G., Belov, B. A., Levitin, A. E., Markova, M. Yu. & Feldstein, Y. I. 1979b Correlation model of the field-aligned currents in high latitudes (summer 1968, maximum of the solar activity), IZMIRAN preprint no. 11(240), Moscow.
- Akasofu, S.-I. 1977 *Physics of magnetospheric substorms*. Dordrecht: Reidel.
- Akasofu, S.-I. 1979a *Planet. Space Sci.* **27**, 425.
- Akasofu, S.-I. 1979b *Planet. Space Sci.* **27**, 1055.
- Akasofu, S.-I. 1979c *Q. Jl R. astr. Soc.* **20**, 119.
- Antonova, E. E. 1979 *Geomagn. Aeronom.*, **19**, 676.
- Arnoldy, R. L. 1971 *J. geophys. Res.* **76**, 5189.
- Axford, W. I. 1964 *Planet. Space Sci.* **12**, 45.
- Axford, W. I. 1969 *Rev. Geophys. Space Phys.* **7**, 421.
- Axford, W. I. 1979 Private communication.
- Axford, W. I. & Hines, C. O. 1961 *Can. J. Phys.* **39**, 1433.
- Belov, B. A., Afonina, R. G., Levitin, A. E. & Feldstein, Y. I. 1977 In *Variations of the magnetic field and the aurora*, p. 15. Moscow: Nauka.
- Boström, R. 1964 *J. Geophys. Res.* **69**, 4983.
- Boström, R. 1974 In *Magnetospheric physics* (ed. B. M. McCormac), p. 45. Dordrecht: Reidel.
- Boström, R. 1975 In *Physics of the hot plasma in the magnetosphere* (ed. B. Hultqvist & L. Stenflo), p. 341. New York: Plenum Press.
- Burch, J. L. & Heelis, R. A. 1979 In *Dynamics of the magnetosphere* (ed. S. I. Akasofu), p. 121. Dordrecht: Reidel.
- Burke, W. J., Kelley, M. C., Sagalyn, R. G., Smiddy, M. & Lai, S. T. 1979 *Geophys. Res. Lett.* **6**, 21.
- Burrows, J. R., McDiarmid, I. B. & Wilson, M. D. 1978 *Transverse geomagnetic field perturbations near the daytime cleft due to Birkeland currents and their relationship to charged particle fluxes and the IMF*, S.T.P. Symposium, Innsbruck. (Preprint.)
- Burrows, J. R., Wilson, M. D. & McDiarmid, I. B. 1976 In *Magnetospheric particles and fields* (ed. B. M. McCormac), p. 111. Dordrecht: Reidel.
- Burton, R. K., McPherron, R. L. & Russell, C. T. 1975 *J. geophys. Res.* **80**, 4204.
- Caan, M. N., McPherron, R. L. & Russell, C. T. 1977 *J. geophys. Res.* **82**, 4837.
- Cattell, C., Lysak, R., Torbert, R. B. & Mozer, F. S. 1979 *Geophys. Res. Lett.* **6**, 621.
- Coleman, P. J. & McPherron, R. L. 1970 In *Particles and fields in the magnetosphere* (ed. B. M. McCormac), p. 171. Dordrecht: Reidel.
- Crooker, N. V. 1979 *J. geophys. Res.* **84**, 951.
- Cummings, W. D., Barfield, J. N. & Coleman, P. J. 1968 *J. geophys. Res.* **73**, 6687.
- Dungey, I. W. 1961 *Phys. Rev. Lett.* **6**, 47.
- Fairfield, D. H. & Ness, N. F. 1972 *J. geophys. Res.* **77**, 611.
- Fairfield, D. H. 1973 *J. geophys. Res.* **78**, 1535.
- Fairfield, D. H. 1977 *Rev. Geophys. Space Phys.* **15**, 285.
- Fairmark, D. S., Krylov, A. L., Levitin, A. E. & Feldstein, Y. I. 1976 In *Solar wind and the magnetosphere*, p. 47. Moscow: IZMIRAN.
- Feldstein, Y. I. 1976 *Space Sci. Rev.* **18**, 777.
- Feldstein, Y. I., Levitin, A. E., Afonina, R. G. & Belov, B. A. 1982 Magnetosphere-ionosphere coupling. (In the press.)
- Foster, J. C., Fairfield, D. H., Ogilvie, K. W. & Rosenberg, T. J. 1971 *J. geophys. Res.* **76**, 6971.
- Friis-Christensen, E. 1979 In *Magnetospheric study 1979*, p. 290. Tokyo: Japan I.M.S. Committee.
- Friis-Christensen, E., Lassen, K., Wilhjelm, J., Wilcox, J. M., Gozalez, W. & Colburn, D. S. 1972 *J. geophys. Res.* **77**, 337.
- Friis-Christensen, E. & Wilhjelm, J. 1975 *J. geophys. Res.* **80**, 1248.
- Fujii, R. & Iijima, T. 1979 *Antarctic Res.* no. 63, p. 232.
- Gurevich, A. V., Krylov, A. L. & Tsedilina, E. E. 1976 *Space Sci. Rev.* **19**, 59.
- Hirshberg, J. & Holzer, T. E. 1975 *J. geophys. Res.* **80**, 3553.
- Horwitz, J. L. & Akasofu, S.-I. 1979 *J. geophys. Res.* **84**, 2567.
- Iijima, T., Fujii, R. & Potemra, T. A. 1979 In *Magnetospheric study 1979*, p. 41. Tokyo: Japan IMS Committee.
- Iijima, T., Fujii, R., Potemra, T. A. & Saffekos, N. A. 1978 *J. geophys. Res.* **83**, 5595.
- Iijima, T. & Potemra, T. A. 1976a *J. geophys. Res.* **81**, 2165. (I.P. 1976a).
- Iijima, T. & Potemra, T. A. 1976b *J. geophys. Res.* **81**, 5971. (I.P. 1976b).

- Iijima, T. & Potemra, T. A. 1978 *J. geophys. Res.* **83**, 599. (I.P. 1978).
- Ivanov, K. G. & Mikerina, N. V. 1973 *Geomagn. Aeron.* **13**, 412.
- Ivanov, K. G. & Mikerina, N. V. 1974 In *Solar wind and the magnetosphere*, p. 3. Moscow: IZMIRAN.
- Iwasaki, N. & Nishida, A. 1967 *Rep. Ionos. Space Res. Japan*, **21**, 17.
- Iyemori, T., Maeda, H. & Kamei, T. 1979 *J. Geomagn. Geoelectr.* **31**, 1.
- Jaggi, R. K. & Wolf, R. A. 1973 *J. geophys. Res.* **78**, 2852.
- Kamide, Y. 1979 *Antarctic Record* no. 63, 61.
- Kamide, Y. & Akasofu, S.-I. 1974 *J. geophys. Res.* **79**, 3755.
- Kamide, Y. & Brekke, A. 1975 *J. geophys. Res.* **80**, 587.
- Kamide, Y. & Matsushita, S. 1979a *J. geophys. Res.* **84**, 4083.
- Kamide, Y. & Matsushita, S. 1979b *J. geophys. Res.* **84**, 4099.
- Kane, R. P. 1976 *Space Sci. Rev.* **18**, 413.
- Kawasaki, K., Yasuhara, F. & Akasofu, S.-I. 1973 *Planet. Space Sci.* **21**, 1743.
- King, J. H. 1975 *I.M.F. date book*, NSSDC, Goddard Space Flight Center, Greenbelt, Maryland.
- Kuznetsov, B. M. & Troshichev, O. A. 1977 *Planet. Space Sci.* **25**, 15.
- Langel, R. A. 1975 *J. geophys. Res.* **80**, 1261.
- Leontjev, S. V. & Lyatsky, V. B. 1980 *Geomagn. Aeron.* **20**, 439.
- Levitin, A. E., Belov, B. A., Afonina, R. G. & Feldstein, Y. I. 1977 In *Variations of the magnetic field and the aurora*, p. 110. Moscow: IZMIRAN.
- Lyatsky, V. B. 1978 *The current systems of magnetospheric-ionospheric disturbances*. Leningrad: Nauka.
- Lyatsky, V. B. & Maltsev, Yu. P. 1972 In *Geophysical researches in the auroral zone* (ed. S. I. Isaev) Apatites, p. 74.
- Lyatsky, V. B. & Maltsev, Yu. P. 1975 *Geomagn. Aeron.* **15**, 118.
- Lyatsky, V. B., Maltsev, Yu. P. & Leontjev, S. V. 1974a *Planet. Space Sci.* **22**, 1231.
- Lyatsky, V. B., Leontjev, S. V. & Maltsev, Yu. P. 1974b In *The high-latitude geophysical phenomena* (ed. S. I. Isaev), p. 115. Leningrad: Nauka.
- Maezawa, K. 1976a *J. geophys. Res.* **81**, 2289.
- Maezawa, K. 1976b In *Physics of solar planetary environments* (ed. D. J. Williams), Publ. Am. Geophys. Union, 608.
- Maezawa, K. 1978 *Solar terr. environ. Res. Japan*, **2**, 103.
- Mansurov, S. M. 1969 *Geomagn. Aeron.* **9**, 622.
- Mansurov, S. M. & Mansurova, L. G. 1973 *J. geophys. Res.* **78**, 2064.
- McDiarmid, I. B., Budzinski, E. E., Wilson, M. D. & Burrows, J. R. 1977 *J. geophys. Res.* **82**, 1513.
- McDiarmid, I. B., Burrows, J. R. & Wilson, M. D. 1978a *J. geophys. Res.* **83**, 681.
- McDiarmid, I. B., Burrows, J. R. & Wilson, M. D. 1978b *J. geophys. Res.* **83**, 5753.
- McDiarmid, I. B., Burrows, J. R. & Wilson, M. D. 1979 *J. geophys. Res.* **84**, 1431.
- McDiarmid, I. B., Burrows, J. R. & Wilson, M. D. 1980 *J. geophys. Res.* **85**, 1163.
- McPherron, R. L., Russell, C. T. & Aubry, M. P. 1973a *J. geophys. Res.* **78**, 3131.
- McPherron, R. L., Russell, C. T., Kivelson, M. G. & Coleman, P. J. 1973b *Radio Sci.* **8**, 1059.
- Meng, C.-I. & Akasofu, S.-I. 1969 *J. geophys. Res.* **74**, 4035.
- Meriwether, J. W., Heppner, J. P., Stolarik, J. D. & Westcott, E. M. 1973 *J. geophys. Res.* **78**, 6643.
- Mishin, V. M. 1977 *Space Sci. Rev.* **19**, 621.
- Mishin, V. M. 1978 *Geomagn. Aeron.* **18**, 961.
- Mishin, V. M. 1979 Private communication.
- Mozer, F. S., Cattell, C. A., Hudson, M. K., Lyzak, R. L., Temerin, M. & Torbert, R. 1980 *Space Sci. Rev.* **27**, 155.
- Mozer, F. S., Gonzales, W. D., Bogott, F., Kelley, M. C. & Schultz, S. 1974 *J. geophys. Res.* **79**, 56.
- Nishida, A. 1968 *J. geophys. Res.* **73**, 5549.
- Nishida, A. 1971 *Cosmic Electrodyn.* **2**, 350.
- Nishida, A. 1975 *Space Sci. Rev.* **17**, 353.
- Nishida, A. 1978 *Geomagnetic diagnosis of the magnetosphere*. Berlin: Springer.
- Nishida, A. & Kokubun, S. 1971 *Rev. Geophys. Space Phys.* **9**, 417.
- Perreault, P. D. & Akasofu, S.-I. 1978 *Geophys. Jl. R. astr. Soc.* **54**, 547.
- Potemra, T. A. 1979 *Rev. Geophys. Space Phys.* **17**, 640.
- Potemra, T. A., Iijima, T. & Safflekos, N. A. 1979 In *Dynamics of the magnetosphere* (ed. S. I. Akasofu), p. 165. Dordrecht: Reidel.
- Pudovkin, M. I. 1974 *Space Sci. Rev.* **16**, 727.
- Pudovkin, M. I. 1975 In *Substorms and disturbances in the magnetosphere* (ed. S. I. Isaev), p. 3. Leningrad: Nauka.
- Pudovkin, M. I. & Semenov, V. S. 1977 *Ann. Geophys.* **33**, 423.
- Rezhnev, B. V., Lyatsky, V. B. & Maltsev, Y. P. 1980 *Planet. Space Sci.* **28**, 595.
- Rostoker, G. 1978 *J. Geomagn. Geoelect., Kyoto* **30**, 67.
- Rostoker, G., Armstrong, J. C. & Zmuda, A. J. 1975 *J. geophys. Res.* **80**, 3571.
- Rostoker, G. & Boström, R. 1976 *J. geophys. Res.* **81**, 235.
- Russell, C. T. 1971 *Cosmic Electrodyn.* **2**, 184.
- Russell, C. T. 1973 *Space Sci. Rev.* **15**, 205.

GEOMAGNETIC VARIATIONS AND FIELD-ALIGNED CURRENTS 301

- Russell, C. T. & Rosenberg, R. L. 1974 *Sol. Phys.* **37**, 251.
- Saflekos, N. A., Potemra, T. A. & Iijima, T. 1978 *J. geophys. Res.* **83**, 1493.
- Saflekos, N. A., Potemra, T. A., Kintner, P. M. & Green, J. L. 1979 *J. geophys. Res.* **84**, 1391.
- Sergeev, V. A. 1977 *Phys. Solariterr.* no. 4, 19.
- Shelomentsev, V. V. & Suche-Bator, U. 1976 In *Researches on the geomagnetism, aeronomie and physics of the Sun*, vol. 39, 128. Irkutsk: Nauka.
- Stern, D. P. 1973 *J. geophys. Res.* **78**, 7292.
- Stern, D. P. 1977 *Rev. Geophys. Space Phys.* **15**, 156.
- Sugiura, M. 1975 *J. geophys. Res.* **80**, 2057.
- Sugiura, M. 1976 *J. geophys. Res.* **81**, 2155.
- Sumaruk, P. V. & Feldstein, Y. I. 1973 *Cosmicheskie Issledovaniya*, **11**, 155.
- Sumaruk, P. V. & Feldstein, Y. I. 1975 *Usp. Fiz. Nauk*, **116**, 344.
- Sumaruk, P. V. & Feldstein, Y. I. 1977 *Astron. Vestn.* **11**, 64.
- Sumaruk, P. V., Feldstein, Y. I. & Shevnina, N. F. 1974 *Geomagn. Aeron.* **14**, 1069.
- Svalgaard, L. 1968 *Geophys. Pap.* R-6, Danish Meteorological Institute, Charlottenlund, Denmark.
- Svalgaard, L. 1973 *J. geophys. Res.* **78**, 2064.
- Svalgaard, L. 1977 In *Coronal holes and high speed streams* (ed. J. P. Zirker), p. 371. Colorado Associated University Press.
- Troshichev, O. A. 1975 In *Substorms and disturbances in the magnetosphere* (ed. S. I. Isaev), p. 66. Leningrad: Nauka.
- Troshichev, O. A. & Tsiganenko, N. A. 1979 In *Geomagnitnija Issledovaniya*, no. 25, p. 47. Moscow: Soviet Radio.
- Troshichev, O. A., Vasiljev, V. P. & Kuznetsov, B. M. 1979 In *Geomagnitnija Issledovaniya*, no. 26, p. 62. Moscow: Soviet Radio.
- Tverskoy, B. A. 1968 In *Dynamics of the radiation belts*. Moscow: Nauka.
- Vasiliunas, V. M. 1970 In *Particles and fields in the magnetosphere* (ed. B. M. McCormac), p. 60. Dordrecht: Reidel.
- Vasiliunas, V. M. 1972 In *Earth's magnetospheric processes* (ed. B. M. McCormac), p. 29. Dordrecht: Reidel.
- Volland, H. 1973 *J. geophys. Res.* **78**, 171.
- Volland, H. 1975 *Ann. Geophys.* **31**, 154.
- Wilhjelm, J., Friis-Christensen, E. & Potemra, T. A. 1978 *J. geophys. Res.* **83**, 5586.
- Wolf, R. A. 1970 *J. geophys. Res.* **75**, 4677.
- Wolf, R. A. 1974 In *Magnetospheric physics* (ed. B. M. McCormac), p. 167. Dordrecht: Reidel.
- Wolf, R. A. 1975 *Space Sci. Rev.* **17**, 537.
- Yasuhara, F., Kamide, Y. & Akasofu, S.-I. 1975 *Planet. Space Sci.* **23**, 1355.
- Zmuda, A. J., Armstrong, J. C. & Heuring, F. T. 1970 *J. geophys. Res.* **75**, 4757.
- Zmuda, A. J. & Armstrong, J. C. 1974 *J. geophys. Res.* **79**, 4611.